Neuromorphic
Computing and
Engineering

TOPICAL REVIEW • OPEN ACCESS

Retinomorphic devices beyond silicon for dynamic machine vision

NEUROMORPHIC
Computing and Engineering

TOPICAL REVIEW

Retinomorphic devices beyond silicon for dynamic machine vision

Yuxin Xia[1,*], Roshni Satheesh Babu[1], Sujaya Kumar Vishwanath[1] and Dimitra G Georgiadou[1,2,*]

[1] Centre for Neuromorphic Technologies, School of Electronics and Computer Science, University of Southampton, Highfield Campus, Southampton SO17 1BJ, United Kingdom
[2] Optoelectronics Research Centre, University of Southampton, Highfield Campus, Southampton SO17 1BJ, United Kingdom
[*] Authors to whom any correspondence should be addressed.

E-mail: y.xia@soton.ac.uk and d.georgiadou@soton.ac.uk

Keywords: neuromorphic, retinomorphic, perovskites, metal oxides, 2D materials, organic materials

OPEN ACCESS

RECEIVED
1 July 2025

REVISED
9 November 2025

ACCEPTED FOR PUBLICATION
19 November 2025

PUBLISHED
5 December 2025

Abstract

The human visual system can effectively sense optical information through the retina and process it at the visual cortex. Compared with conventional machine vision, it demonstrates superiority in terms of energy efficiency, adaptability, and accuracy. The retina-inspired machine vision systems can process information near or within the sensors at the front end, thereby compressing the raw sensory data and optimising the input to back-end processor for high-level computing tasks. In recent years, amid surge of interest in artificial intelligence technology, research in retinomorphic devices has achieved breakthroughs in both academic and industrial settings. Herein, we present a comprehensive review of this emerging field -based on several materials classes, such as halide perovskites, two-dimensional materials, organic materials and metal oxides. We discuss the steps taken towards achieving not only static pattern recognition, but also dynamic motion tracking and we identify the key challenges that need to be addressed by the community to push this technology forward.

1. Introduction

The term 'retinomorphic' is derived from the biological retina, the light-sensitive layer at the back of the human eye responsible for converting light into neural signals. In the context of optoelectronics and neuromorphic engineering, retinomorphic devices are engineered systems that mimic the structure and/or functionalities of the biological retina. The latter serves as an exemplary model for creating efficient, low-power, and high-speed optoelectronic systems.

Retinomorphic devices aim to replicate the retina's ability to receive and transduce visual information in a highly efficient and parallel manner. The genesis of retinomorphic devices can be tracked back to the early explorations in neuromorphic engineering in the late 1980s. The first attempts at incorporating retinal functions into analogue silicon circuits were centred on the work led by Carver Mead [1–3], whose group established and fabricated motion detecting circuits using principles found in the human eye, such as the centre-surround spatial derivative mechanism. Later, implementations based on silicon intended for image recognition [4], edge detection [5], image Boolean processing [6], and local adaptation to varied background intensity [7, 8] have been studied in both device and system architectures as well as in algorithmic approaches.

In the era of big data, the massive influx of information and increasingly complex external environments demand more advanced multi-functional artificial intelligence (AI) chips. Since visual perception plays a key role in gathering environmental information, there is a growing need for devices that can sense, store, and process visual data with higher speed, greater efficiency, and reduced power consumption. While traditional machine vision technology has significantly impacted various aspects of human life, such as industrial automation of parts inspection and assembly, it is becoming increasingly inadequate for more complex tasks, like real-time object recognition and fast decision-making that is required in autonomous vehicles, due to limitations in current computing architectures, known as the von Neumann bottleneck. As a result, developing smarter machine vision technologies to meet today's

evolving demands has become a crucial area of innovation in the post-Moore's Law era [9]. Meanwhile, the evolution of retinomorphic devices has been significantly influenced by advancements in materials science, particularly through the development of novel semiconductors, memristive devices, and nanostructured components [10–12]. In this review, we will summarise recent developments with novel device architectures and materials classes other than silicon that are attractive for this emerging application field.

2. Biological principles

The human eye, a miracle of nature's engineering, exhibits remarkable capability that surpasses current technological counterparts in several aspects. The primary functions of the human visual system can be categorised into two aspects: image perception and pre-processing, which occur in the eye, and recognition and memory processing, which take place in the cerebral cortex's visual centre [13]. Its ability to process vast amounts of visual information with minimal energy consumption, adapt to varying light conditions, and perform real-time image processing are key features that inspire technological innovation [14].

2.1. The function of the biological retina

Light from the environment, including that reflected from external objects, enters the eye through the pupil and passes through the crystalline lens, where it is refracted before reaching the retina. The retina has the remarkable ability to convert light stimuli into electrical signals, which forms the basis for visual perception in living organisms. This process is highly efficient due to the optically superior and structurally compact design of the natural vision system. Key attributes of this system include high sensitivity, high resolution, a wide field of view, and a broad colour gamut [15]. Its superiority roots on the various cells that compose the retina, each contributing uniquely to the perception, processing and transmission of visual information [15–18]. Understanding these functionalities of retina cells is of prime importance for designing retinomorphic devices that accurately emulate biological vision. The retina itself has a well-defined hierarchical structure, which consists of five main types of cells, namely photoreceptors, horizontal, bipolar, amacrine, and ganglion cells, as shown in figure 1(A).

(a) There are two types of photoreceptors, i.e. rods, and cones (figure 1(B)). Rods are specialised for low-light (scotopic) vision and essential for night vision and peripheral vision. Rods have high sensitivity to light but do not contribute to colour perception. Cones are responsible for colour vision and visual acuity, and function optimally in bright light conditions (photopic). There are three types of cones, each sensitive to different wavelength, corresponding to red, green, and blue light.
(b) Bipolar cells serve as intermediates between photoreceptors and ganglion cells. They receive input from multiple photoreceptors and transmit the processed signals to ganglion cells, playing a crucial role in signal amplification and integration.
(c) Amacrine and horizontal cells are laterally intensive interneurons in the inner and outer retina, respectively. General functions attributed to amacrine cells include surround inhibition, some forms of adaptation, signal averaging, and noise reduction [19, 20], while, horizontal cells are believed to be responsible for perceiving the low-contrast details under bright light [21]. Through regulation of amacrine cells, redundant and unstructured data are filtered out, leaving only the refined visual data being transmitted [18].
(d) Ganglion cells are the final output neurons of the retina, whose axons form the fibres of the optic nerve. They receive input from bipolar and amacrine cells and transmit visual information to the brain via the optic nerve. Ganglion cells are responsible for encoding information regarding light intensity, colour, motion, and central-surround contrast [13].

Recent research has revealed a greater diversity of retinal cell types and subtypes than previously understood, with many of their distinct roles and functionality still under investigation [24]. However, there is a consensus on some fundamental roles they play in visual processing. The principal functional categories of retinal cells can be summarised as follows [25]:

(a) Sensitivity to light transients: Certain retinal cells are highly responsive to transient changes in light intensity. This transient sensitivity enables quick visual detection, contributing to motion perception and alerting the visual system to dynamic changes in the environment.

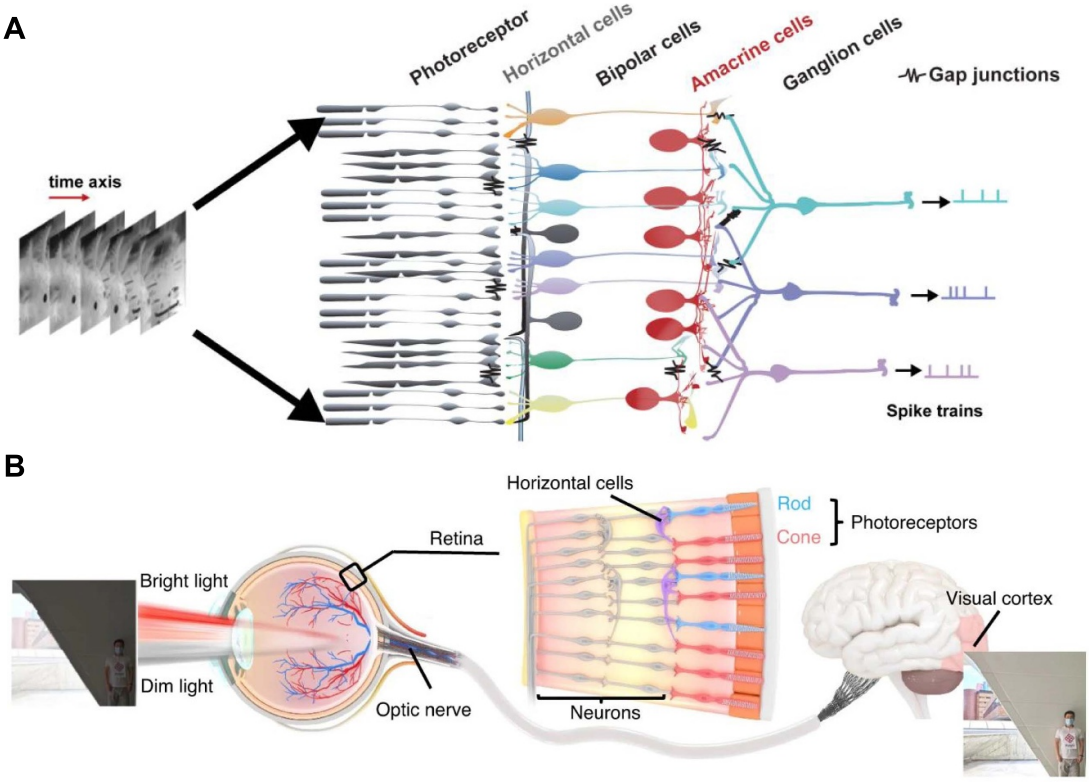

Figure 1. (A) Schematic diagram of the retinal circuit. Reproduced from [22]. CC BY 4.0. (B) The retina adapts to different illumination intensities through photoreceptors (including cones and rods) and horizontal cells. The objects under extreme light conditions can be well perceived for accurate representation by visual adaptation. Reproduced from [23], with permission from Springer Nature.

(b) Adaptability to sustained luminance: Other retinal cells are adaptive to sustained levels of ambient luminance, or ongoing light intensity. These cells help regulate visual responses based on background light levels, adapting the sensitivity of other retinal neurons accordingly.

(c) Sensitivity to direction of motion: Some retinal cells, particularly certain types of ganglion cells, are specialised in detecting the direction of motion. These directionally selective cells respond preferentially to movement in specific directions across the retina, providing the brain with important information about the trajectory of moving objects.

(d) Sensitivity to spatial contrast (centre-surround antagonism): A key aspect of retinal processing is spatial contrast sensitivity, which arises from the centre-surround antagonistic organisation of receptive fields in the retina. This arrangement enables the detection of edges, borders, and fine details within the visual scene by highlighting contrasts between light and dark regions.

2.2. Biomimetic imager

Inspired by the optical sophistication of biological eyes, researchers have been developing artificial systems that replicate these essential sensing functions by achieving innovations in imaging optics, bioinspired lenses, light filtering components, and adjustable apertures. In retinomorphic devices, emulation of these functionalities involves replicating the processes of signal detection, processing, and transmission. Photoreceptors are typically emulated by photodetectors, bipolar cells by signal amplifiers or integrators, and ganglion cells by output transducers or neural interfaces. Advanced and emerging retinomorphic systems also strive to incorporate lateral and feedback mechanisms analogous to horizontal and amacrine cells to extend image processing and computing capabilities, such as edge detection, motion sensing and pattern recognition. Despite these advances, challenges remain, particularly in replicating the full range of the biological eye's capabilities, such as its seamless adaptability and durability [26–32]. Together with the development of optical/photonic fabrication techniques, it is expected that tailored optical components in artificial vision systems will enable efficient future machine vision.

In this review, we focus on the advancements made in image processing and computation tasks rather than sensing.

3. Retinomorphic optoelectronic devices for machine vision

The study of the retina has inspired the development of advanced machine vision that mimics the human visual system with the aim to combine functions, including imaging, processing, and visual information storing in a way that responds quickly to complex environments [33–38]. The novel retinomorphic systems exhibit obvious performance improvement compared with traditional complementary metal–oxide–semiconductor (CMOS)-based machine vision systems [39].

The pre-processing occurring at the retina reduces the burden on the brain's visual cortex and accelerates cognitive processes [17]. Depending on whether the image sensors can perform *in-situ* pre-processing or not, retinomorphic vision systems can be divided into two types: homogeneous and heterogeneous, respectively (figure 2).

In the heterogeneous configuration, the image sensors are only responsible for sensing and the visual information obtained by them is further transmitted to processing units. In some contexts, peripheral control units are also needed to change the sensors' states and output in a predefined way to achieve pre-processing [5, 40]. The processing units could be near-sensor or peripheral, executing specific signal pre-processing (data compressing and filtering, local gain adaptation) to mimic retina's functionality. A more ambitious attempt is to integrate an artificial neural network (ANN) hardware that reproduces the ability of visual cortex to perform image recognition and objects tracking. The heterogeneous architecture is advantageous for tasks requiring high adaptability and cognitive functions, as it separates the data acquisition and processing phases, allowing each component to specialise in its respective functions [41]. One direction of research focus of heterogeneous integration is on the design of peripheral computing units, aiming at both hardware and algorithmic innovations. Another approach is to develop near-sensor monolithic devices that offer first-stage processing of the signal received from sensor, such as compressing, filtering and storing, leveraging the unique analogue non-linearity of emerging materials or device architectures [42].

A homogeneous system integrates pre-processing capabilities directly within the image sensors. This integration can lead to faster processing, and reduced latency, since initial data processing is performed *in-situ*. In addition, by removing near-sensor/peripheral processing units, this integration could be more energy efficient and compact. Integrating computing capabilities with sensors demands careful design, considering the sensors' dynamics. As the computing process unfolds, the states of the sensors may change, affecting their ability to accurately sense the environment. This dynamic interplay requires a sophisticated approach to ensure that the sensing and computing work in harmony. Successful integration means designing systems that can adapt to these changes without compromising performance or efficiency.

It is important to note that the proposed classification framework is not rigid and may not be universally applicable to all device configurations. For instance, consider a sensor that is electrically connected to and physically proximal to a memristive device [43]. Such memristive devices, which may be as simple as a capacitor or a memristor, together with the sensors appearing as one integration, present an interesting classification challenge. The distinction is intuitive and context-dependent, often influenced by the specific architectural and functional relationships between the components. In this study, for consistency and clarity, we classify such configurations as heterogeneous integration.

It should be also noted, that retinomorphic devices, in a broader sense, include any hardware implementation inspired by the principles of retinomorphic signal processing. These devices are not limited to incorporating photo-sensors specifically. Instead, they focus on the processing of spatial and temporal sensory information, which can extend beyond just visual data [3, 38, 44–47]. As such, these devices can handle various types of information, improving their versatility and application scope. This approach allows for innovative uses in fields where diverse sensory inputs must be processed efficiently, leveraging the retinomorphic paradigm beyond traditional visual systems.

3.1. Heterogeneous integration

The implementation of vision system at its early stage was mostly based on the heterogeneous paradigm incorporating silicon-based technologies fabricated with CMOS techniques [7, 8, 48–50]. The pioneering works by the Mead lab focused on the design of dynamically configurable analogue circuits together with photosensors, particularly suitable for retinomorphic computing [7, 8, 48, 51]. The active elements were constructed with numerous transistors and resistors that receive signal from and send feedback to the sensors. These systems were more sensitive to either temporal or spatial changes than the constant background and introduced the address-event-representation (AER) communication protocol. By enhancing

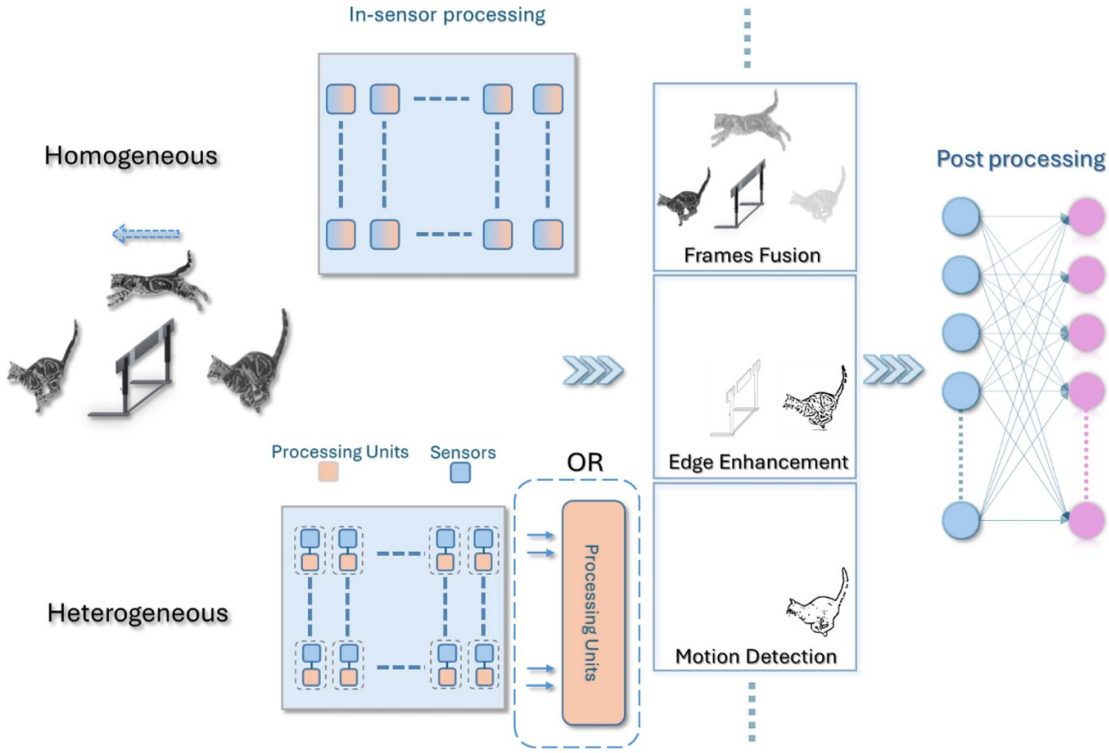

Figure 2. Schematic of homogeneous and heterogeneous configurations. In the homogeneous configuration, both light signal sensing and the first stage of processing occur within the sensors through the state switching of the sensors themselves. In the heterogeneous configuration, sensors are solely dedicated to sensing and outputting data to processing units, which could be simple circuits located near the sensors or peripheral processing units. The processing performed in both configurations typically encompasses a range of operations, including sensing adaptation, image convolution tasks, such as noise removal and edge enhancement, as well as image storage. These processes serve to compress the raw sensory data and extract critical features, thereby optimising the input for subsequent stages of post-processing.

features at finer spatial and temporal scale, facial recognition was made easier [52] and provided spatiotemporal reference for motion tracking. These systems, thus, represented an early step in creating more sophisticated image processing technologies, mimicking the biological retina.

Another type of retinomorphic system was developed in the early nineties by Lange *et al* [5], which consisted of a 64 × 64 array of photodiodes and a peripheral control unit. By sending binary voltages to each row, the control unit manipulated the photodiodes in the same row to exhibit either positive or negative photosensitivity. This adaptability was crucial for implementing simple convolution kernels, which are fundamental operations in image processing. When combined with a neural network, complex tasks, such as image compression and character recognition, can be effectively executed. Unlike the pioneering work of Mead, where near-sensor adaptive circuitry played a central role, system's design shifts the emphasis towards algorithmic innovation and neural network integration rather than hardware adaptability near the sensor. Although the neural network model in most studies was implemented through a standard computer (i.e. based on the von Neumann architecture), rather than a hardware-based neuromorphic processor, at present efforts to merge retinomorphic sensors with neuromorphic processors have been persistent. This persistence is unsurprising, given the growing interest in neuromorphic computing.

Neuromorphic computing, inspired by breakthroughs in neuroscience, represents a revolutionary computational paradigm that emulates the structural and functional properties of neural circuits in the brain. This approach seeks to replicate the brain's efficiency, adaptability, and parallel processing capabilities, promising a solution to the memory-computation bottleneck found in traditional von Neumann architectures [3, 10, 53]. Neuromorphic devices have already demonstrated remarkable potential, particularly in terms of energy efficiency. In conventional computing systems, a substantial amount of energy is consumed by the transfer of redundant data between sensors, memory, and processors. Neuromorphic devices, by performing front-end pre-processing of raw data, inherently reduce these energy costs. Yao *et al* for example, showed that electronic synapses could operate with 1000 times less energy than an Intel Xeon Phi processor, while performing similar facial recognition tasks [39].

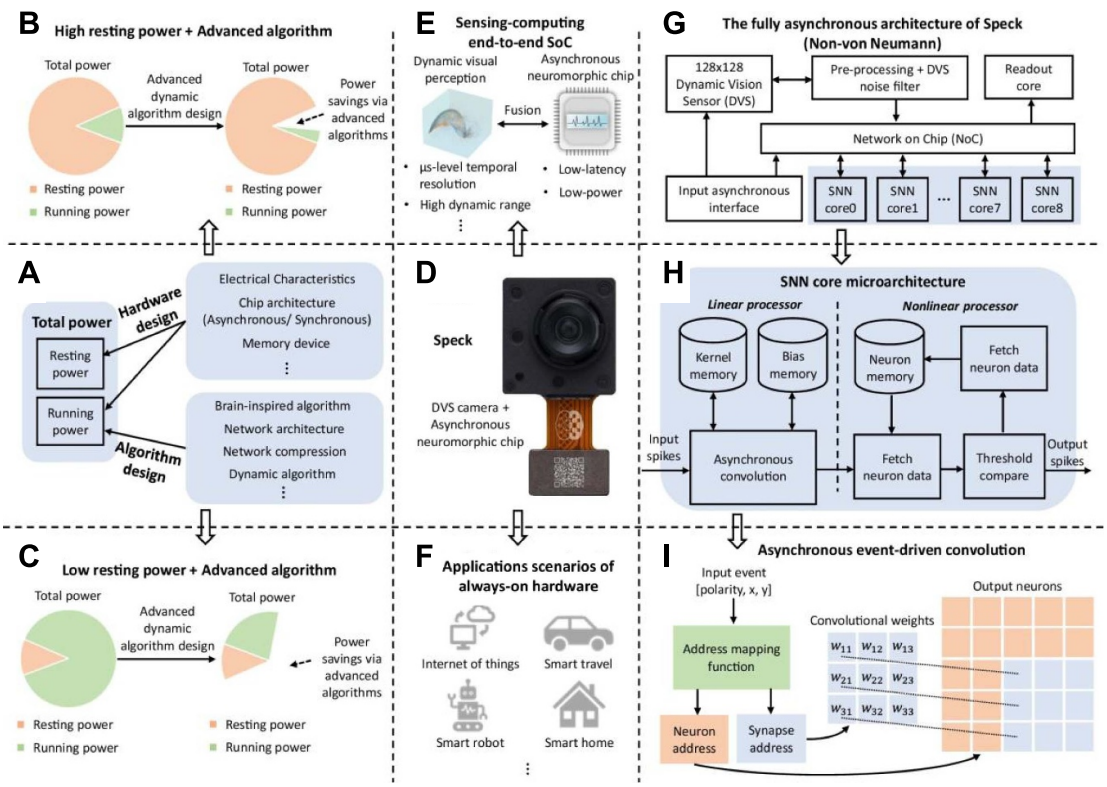

Figure 3. (A) The power composition of AI systems. (B) The case of high resting power. High resting power cannot be compensated by the gain by the advanced algorithm. (C) The case of low resting power. Low resting power helps unleash the power of advanced algorithm design. (D) Speck physical display, smaller than a one-pound coin. (E) Speck integrates a DVS and a neuromorphic chip. (F) Typical application scenarios of Speck. (G)–(H) The fully asynchronous architecture of Speck. The DVS events come from the on-chip sensor. After an asynchronous event pre-processing core, events can be routed to SNN cores for processing. Each SNN core can be simply considered as a spiking convolution layer with an integrated pooling layer. (I) Asynchronous event-driven convolution. Reproduced from [57]. CC BY 4.0.

A heterogeneous architecture that integrates sensors with neuromorphic devices has emerged as a significant approach for enhancing the efficiency of visual information processing. This integration has the potential to optimise system performance and reduce latency and energy consumption [43, 54–56]. With the progression of neuromorphic hardware, a hardware implementation of a comprehensive sensing-processing-learning-actuating system, known as CAVIAR, was demonstrated in 2009 [50]. The CAVIAR system incorporates a sensor array, convolution chips, and neural network chips to create a complete machine vision system. With 45 000 neurons and 5 million synapses, the system can perform approximately 12 billion synaptic operations per second, demonstrating the potential of neuromorphic hardware to revolutionise real-time image processing and computational efficiency in machine vision applications.

The latest breakthrough is a sensing-computing neuromorphic system on chip (SoC) known as 'Speck' (figure 3), which was developed by SynSense Corporation in 2024 [57]. Speck is claiming to be the world's first fully event-driven neuromorphic vision SoC using the dynamic vision sensing and the spiking neural network (SNN) technology. It integrates a 128 × 128 dynamic vision sensor (DVS) array with asynchronous neuromorphic chip (over 330 000 neurons) all on a die of 6.1 × 4.9 mm, using a 65 nm low-power COMS logic process. Furthermore, it comprises an attention-based dynamic computing framework, which can assist SNN in discriminative regulation of power consumption based on the importance of input. The high integration intensity and new attention-based framework cut the energy consumption to ultra-low levels, with resting power 0.42 mW and real time power less than 5 mW, while maintaining the 0.1 ms latency and high accuracy. For comparison, thousands of times more power (30 W) is needed to achieve same accuracy for the same gesture recognition task performed with same model deployed on general GPUs. Speck represents a notable step toward energy-efficient, dynamic neuromorphic computing, offering a strong foundation for future research and integration into real-world machine vision systems.

3.2. Homogeneous integration

Homogeneous integration refers to a single device designed to exhibit multiple functions, such as image perception, storage, and pre-processing. It switches between different operating modes or states to perform different tasks. The switching could be triggered passively by the signal it is receiving or actively by using control units. Upon embedding functionalities within the sensors, homogeneous systems can efficiently handle tasks, for instance, image memorisation [43], light intensity adaptation [41, 58], edge detection [59], and colour recognition [34].

The key to enable the in-sensor computing is to have configurable and readable states that can be retained. The states' control spans over electric, optic, magnetic, spintronic and ionic. So far, many reports have been published about monolithic optoelectronic devices, which demonstrated switching of the optically activated states, mimicking sensory plasticity of the biologic visual system. Most of them have shown the capability of memory with different retention times ranging from milliseconds [60] to millions of seconds [61], corresponding to short-term and long-term plasticity.

The optical switching has been investigated and applied to memory devices for decades. In 1971, Frohman [62] invented the erasable programmable read-only memory (EPROM), which was the first non-volatile semiconductor memory that was both erasable and reprogrammable, as its name implies, with erasing in EPROM relying on photoelectric effect from UV exposure. Both optical erasing and writing has been attempted in optoelectronic memory devices, with Samorì *et al* introducing in 2017 a non-volatile optical thin-film transistor (TFT) device, capable of achieving over 256 distinct memory states and all-optically controllable writing and erasing [61, 63].

The development of homogeneous integration has been extensively reported in the literature. These devices leverage intrinsic working principles that define their unique architectures and functionalities, often leading to significant variability and complexity. Depending on the predominant working principle, reported studies include phase-change materials, photochromic mechanisms, ferroelectric effects, charge trapping, photo-electrochemical processes, and photo-capacitive effects. Notably, the boundaries between these mechanisms are not strictly defined, with some overlaps occurring, for instance, between phase-change and ferroelectric materials, and between photochromic and photo-electrochemical switching. Furthermore, certain devices integrate multiple mechanisms to enhance performance and efficiency [64]. Representative examples of devices operating under these mechanisms are shown in table 1.

Phase-change material-based memory relies on materials, such as chalcogenide glasses and metal dichalcogenides, utilising reversible phase transitions between amorphous and crystalline states to store information. These transitions occur on sub-nanosecond timescales, offering compatibility and flexibility for optoelectronic applications [78–80]. While most studies emphasise optical properties, such as refractive index variations, for photonic memory devices, some studies have also explored resistance transitions during phase changes, broadening the scope of their applicability [65].

Ferroelectric-based devices utilise polarisation switching and have long been studied for their electrical manipulation capabilities. More recently, the dual optical and electrical control of resistance states has emerged as a critical topic of interest for retinomorphic applications. Two primary device types dominate this field: ferroelectric tunnel junctions (FTJs) and ferroelectric TFTs. Optical control of resistance states in FTJs has been proposed as a highly energy-efficient and ultrafast process, with sub-nanosecond response times [81]. In both types of devices, polarisation can be modulated through photo-excited charge and electric field redistribution, stemming either from the absorption properties of ferroelectric materials themselves, such as α-In_2Se_3 [41] or $BaTiO_3$ [64], or via photosensitive materials in their vicinity [68, 70, 82].

Photochromic materials have traditionally been explored for their optical memory and switching capabilities [83, 84]. Recent research has expanded to investigate their electrical properties [85, 86]. Upon light stimulation, the energetic transitions of photochromic materials can alter overall resistance states when blended with organic semiconductors. For instance, in systems comprising diarylethene (DAE) and poly(3-hexylthiophene) (P3HT), the photo-transition between DAE isomers shifts the HOMO energy level within or outside the P3HT bandgap, creating trapping centres and yielding high-resistance states [61, 63]. A key advantage of photochromic materials is their optically reversible transitions, which can be controlled entirely by optical stimuli, facilitating optical writing and erasing for retinomorphic applications [87, 88].

Photo-electrochemical devices leverage photon-mediated electrochemical reactions, for instance, doping processes in P3HT [74–76], or silver conductive filament formation [73]. Some devices exhibit functional similarities to biological neurons due to their electronic and ionic interactions within electrolytic environments, making them particularly suited for neuromorphic applications.

Charge trapping mechanisms, commonly utilised in floating-gate transistors, have also been adapted for retinomorphic devices. In such devices, charges injected into a trapping layer, tunnelling through

Table 1. Representative examples of retinomorphic devices as per their operating hboxmechanism.

Mechanism	Device structure	Device type	Modulation control	Year	References
Phase Change	ITO/$Ge_2Sb_2Te_5$ (GST)/ ITO	MIM[a]	Voltage: Refractive index, conductance	2014	[65]
	$Ge_2Sb_2Te_5$ (GST)	MIM	Voltage: Refractive index, conductance	2018	[66]
	$Ge_2Sb_2Te_5$ (GST)	MIM *on Metal Heater*	Voltage: Refractive index	2021	[67]
Ferroelectric	P(VDF-TrFE)/Al_2O_3/AZTO	Transistor	Voltage: Transconductance	2010	[68]
	MoS_2 /$BaTiO_3$/ $SrRuO_3$	Diode	Light & voltage: Polarisation	2018	[69]
	STO/$La_{2/3}Sr_{1/3}MnO_3$/ $BaTiO_3$/Pt	MIM	Light: Conductance	2021	[64]
	α-In_2Se_3	Transistor	Light: Transconductance	2022	[41]
	PMMA/C_8-BTBT /P(VDF-TrFE)	Transistor	Light: Transconductance	2024	[70]
Charge Trapping	P3HT:PCBM/PVCN/PDPP3T:PCBM/PVA	Transistor	Voltage & light: Photoresponsivity	2021	[58]
	Ti-Au/ZrO_2/TiN/HZO/TiN/Si	Transistor	Light: Photoresponsivity	2022	[71]
	Al_2O_3/Pt/Al_2O_3/WSe_2	Transistor & Diode	Voltage & light: D–S Conductance, photoresponsivity	2024	[72]
Photo-electrochemical	Ag/ $CsPb_2Br_5$/PVA/FTO	MIM	Voltage & light: Conductance	2021	[73]
	azo-tz-PEDOT:PSS/PBS	ECT[b]	Light: D–S Conductance, absorptance	2023	[74]
	P3HT:PCBM/PEGDA:HMP	ECT	Voltage & light: D–S Conductance	2023	[75]
	PEDOT:PSS/Dyes :Bi_2S_3	ECT	Light: D–S conductance	2024	[76]
Photo-capacitor	ITO/P3HT:PCBM/SiO_2/Si	Diode	Light: Photoresponsivity	2021	[60]
	Ag/Teflon/MoO_3/CDT-TQ:PCBM/SnO_2/ITO	Diode	Light: Photoresponsivity	2023	[77]

[a] MIM: Metal insulator metal

[b] ECT: Electrochemical transistors

a dielectric, remain trapped. Retinomorphic phototransistors extend this architecture by introducing a photosensitive layer between the gate electrode and the trapping layer. Under illumination, photoexcited charges diffuse to the trapping layer and remain trapped, analogous to applying a gate voltage [71, 72]. This architecture also demonstrates photo-capacitive effects due to the existence of dielectric layer [58].

Finally, the photo-capacitive effect has gained attention for its value in retinomorphic applications despite its characteristic slow response time for sensing. The memory retention time in photo-capacitive devices is short but recent studies emphasise its potential in event-triggered sensing, broadening its applicability in functional retinomorphic systems [60, 77].

To explore their full potential as first stage processing unit of a vision system, the integration of sensing arrays with neuromorphic computing units is usually needed to complete some complex tasks, such as pattern recognition and motion tracking. Considering the complexity of scaling up, a small size array of devices is fabricated, or sometimes simulated, based on single device characterisation to serve as a proof of concept. In the study by Park *et al* an ANN was constructed whose 784 synaptic weight connections were simulated based on a single photo-synaptic device. The Modified National Institute of Standards and Technology (MNIST) handwriting recognition task was performed through this ANN, and the recognition rate was found to be improved significantly from 36% to 50% or from 49% to 62%, depending on the number of weight states used in simulation (20 and 100, respectively) [89]. In another work, Liao *et al* fabricated an 8 $\times$ 8 sensor array to demonstrate in-sensor scotopic and photopic adaptations [23]. Experimental results showed enhanced image contrast and accuracy in low (6 μW cm^{-2}) and high (60 mW cm^{-2}) light intensity environments. With a simulated 28 $\times$ 28 sensor array connected to an ANN classifier, the recognition accuracy improved significantly from less than 40% without adaptation, gradually with increased adaptation time to >96% [23]. The concept and main results are presented in figure 4. This research showed the great potential of in-sensor processing in reducing circuitry and complex algorithmic requirements compared to the heterogeneous integration.

4. Materials for retinomorphic devices

Unlike the heterogeneous integration, in which traditional materials like silicon have been dominating, several pioneering homogeneous machine vision technologies based on emerging materials have created breakthroughs, within which two-dimensional (2D) materials, metal halide perovskite (MHP) materials, metal oxides and organic materials attract the most attention and will be discussed below.

4.1. Organic materials

Organic semiconductor materials have been heavily investigated and applied in various optoelectronic areas, for example, photovoltaics, photodetectors and light emitting diodes, due to their unique advantages, such as light weight, flexibility, and bandgap tunability. Organic semiconductors' use in memory devices has attracted particular interest for application in neuromorphic computing due to their higher degree of biocompatibility and responsivity to analytes in biological media [90–93]. In addition, high switching ratios [68] and low operating voltages [94] have been demonstrated, while they also offer the possibility to be integrated onto flexible substrates [95, 96].

As discussed in previous sections, various mechanisms have been proposed in the operation of retinomorphic devices and almost for each mechanism, reports of utilising organic materials could be seen, although with varying roles in the device structure. The majority of such materials, for instance poly(3-hexylthiophene) (P3HT) and 2,7-dioctyl[1]benzothieno[3,2-b][1]benzothiophene (C8-BTBT), have been successfully employed in organic phototransistors [25, 70]. Organic ferroelectric materials, such as polyvinylidene fluoride (PVDF) [82], and electrochemical materials, such as poly(3,4-ethylenedioxythiophene):poly(styrenesulfonate) (PEDOT:PSS) [76], have been combined with other photo-responsive materials for retinomorphic applications. The utilisation of multispectral response of organic materials, where organic materials are only responsible for photopic sensing, is also reported for multi-colour perception [76].

The electronic modulation of conduction states in polyethylene and polypropylene in a simple metal–insulator–metal (MIM) configuration can be traced back to the 1970s [97–99]. The metal ions injected into the organic films introduce impurity bands or tunnelling pathways [100]. The optical modulation of conduction was investigated in early 2000s in systems, such as poly[2-methoxy-5-(2′-ethylhexyloxy)-1,4-phenylene vinylene] (MEH-PPV) [101] and potassium tetracyanoquinodimethane (K-TCNQ) [102], both of which are well-known for their versatile applications in the field of organic electronics. For both materials, states switching was controlled by photochromic reactions, and synergistic functions combining light sensing and switching were demonstrated.

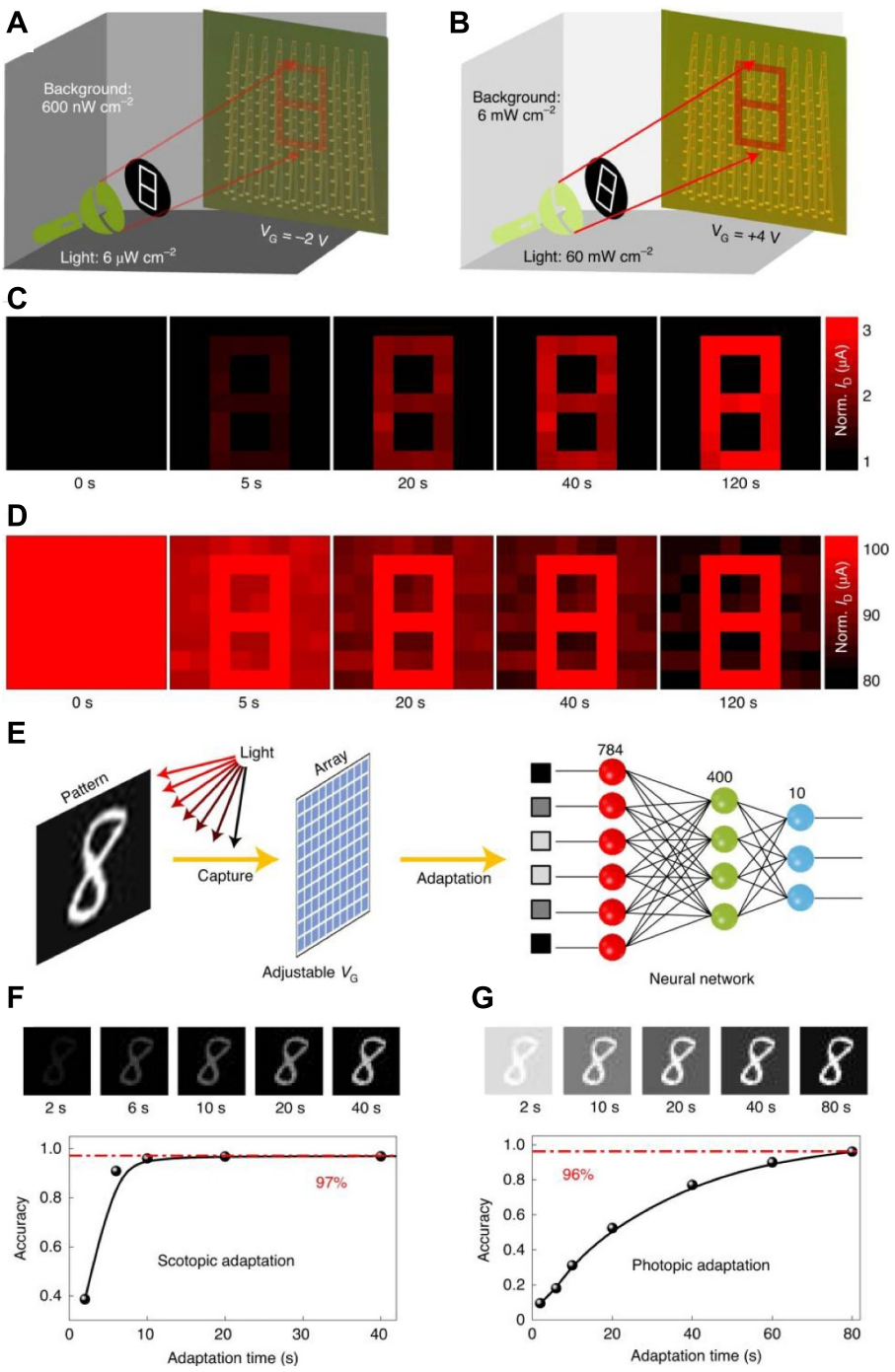

Figure 4. (A)–(B) Schematic of an 8 × 8 array demonstrating the in-sensor (A) scotopic and (B) photopic adaptation under different illumination intensities. (C)–(D) Time courses of the (C) scotopic and (D) photopic adaptation of the digit '8'. (E)–(G) Schematic of simulated 28 × 28 array combined with neural network. MNIST recognition accuracy improved from less than 40% to up to >96% after adaptation. Reproduced from [23], with permission from Springer Nature.

Another champion material, P3HT, which has been playing an important role in the development of organic photovoltaics and transistors in the last two decades [103–105], now finds its position in retinomorphic devices technology. P3HT has high absorption coefficient, spectral response in the visible range and decent carrier mobilities. P3HT has been applied to floating-gate phototransistors [58], photochromic transistors [61], photoelectrochemical devices [75, 96] and photodiodes [60]. A flexible, non-volatile optical TFT device capable of achieving over 256 distinct memory states was developed using a blend of P3HT and a well-studied photochromic molecule, namely diarylethene (DAE) [61, 63]. The device leverages reversible isomerisation of DAE molecules under UV and green light to modulate the conductivity of the blend film, enabling multilevel data storage. In the transistor configuration, its

states could be also modulated electrically; however, its capability for all-optical modulation, UV erasing and green light writing, is apparently more impressive. The authors also demonstrated non-volatility characteristics, with state retention times lasting over 500 d, although endurance is currently limited to 70 write-erase cycles. Interestingly, the mobility of the blend films was found to be dependent on the ratio of the two DAE isomers (open and closed form), changing over several times continuously with increased light dose. This work represents a good example of translating bistable molecules (DAE) into multiple states memory devices by a simple blending strategy, and the ability to control such high number of states presents great potential for neuromorphic computing.

Another example of multiple states was reported by Mei *et al* in 2023, also with a simple architecture [75]. The synaptic weight was modulated by photon mediated electrochemical doping in P3HT:phenyl-C61-butyric acid methyl ester (PCBM) film through protons, H^+. Even though gate voltage dominates the conductance modulation, only small bias below 1 V needs to be applied. The electrochemical doping process mimics ion flux-driven synaptic activities seen in biological systems, allowing for efficient perception, processing, and memorisation of visual information. The synaptic devices demonstrate up to 280 distinct states with excellent reproducibility and stability over more than 10 000 cycles. Furthermore, the devices exhibited short-term and long-term plasticity, adaptive learning, and memory retention, proving their effectiveness in replicating human-like cognitive functions. A prototype array with 18 000 transistors on a 2.5 $\times$ 5.0 cm^2 glass substrate was fabricated, showcasing excellent uniformity in photonic responses. A 64 $\times$ 64 synaptic array was simulated to demonstrate the potential of these devices in constructing artificial retinas capable of facial recognition.

In principle, a wide range of organic semiconductors can be employed in the fabrication of retinomorphic devices, provided they are integrated within a suitably engineered device architecture. One of the most straightforward configurations involves a transistor structure, wherein a multilayer stack of organic materials forms the channel. Within this channel, specific layers are designated for photogeneration of charge carriers, while others serve memory-related functions. For instance, Shao *et al* demonstrated a retinomorphic transistor utilising poly[(9,9-dioctylfluorenyl-2,7-diyl)-co-(4,4′-(N-(4-sec-butylphenyl)diphenylamine)] (TFB) as the photosensitive layer and pentacene as the channel material [106]. TFB exhibits strong ultraviolet (UV) absorption and contributes to charge trapping, enabling the device to exhibit both short-term memory and long-term memory characteristics depending on the UV exposure dose. Prolonged UV illumination leads to a diminished modulation of the device's conductance, effectively mimicking the progressive degradation observed in retinal injury.

Similar transistor-based architectures have been explored using various organic semiconductors. These include indacenodithiophene-benzothiadiazole (IDTBT) and poly[[N,N′-bis(2-octyldodecyl)-naphthalene-1,4,5,8-bis(dicarboximide)-2,6-diyl]-alt-5,5′-(2,2′-bithiophene)] (N2200) [107], poly[2,5-bis(3-tetradecylthiophen-2-yl)thieno[3,2-b]thiophene] (PBTTT) [108], and poly[9,9-dioctylfluorenyl-2,7-diyl-co-bithiophene] (F8T2) [109].

Following the fast progress in neuromorphic computing, researchers have dedicated their efforts not only to optoelectronic performance optimisation at the single device level, but also to the exploration of the integration within neural networks [93]. The goal is then to achieve collaborative innovations from image perception and storage to computing functions to develop new types of human-like vision chips based on organic materials. In 2024, Matrone *et al* developed an end-to-end spiking neural pathway with organic materials [110]. Their circuits were designed to mimic the spiking coding circuitry and the adjustable synaptic plasticity of human nervous system (figure 5). This neuromorphic pathway, combined with a photosensor, is intended to replicate the retina's role as the initial processing stage of visual information, thus allowing signal transmission to resume toward higher-level neural centres.

4.2. Metal oxides

Metal oxides have played a critical role in a new type of non-volatile memory devices, which can be as fast as random-access memory (RAM) but more energy efficient, examples being ferroelectric RAM (FeRAM) based on oxide perovskites, such as $BaTiO_3$ [64] or $PbTiO_3$ [111], and resistive RAM (RRAM) based on transition metal binary oxides. RRAM is a particularly attractive type of memory due to its simple constituents, high density, low power, large endurance, fast write and read speeds and excellent scalability. The dominant mechanisms of RRAM are ion migration and charge trapping [112]. Because of the simplicity of the materials and good compatibility with silicon CMOS fabrication process, research activities have been focused on binary oxides, such as NiO_x, TiO_x, CuO_x, ZnO_x, HfO_x, AlO_x, MoO_x, to name but a few. In 2004 Samsung demonstrated NiO memory array integrated with the 0.18 μm silicon CMOS technology [113]. As to the retinomorphic application, neural networks based on circuits combining CMOS and crossbar resistive memory with Al_2O_3/TiO_{2-x} were developed for pattern recognition in 2015, showing the great potential for scalability of metal oxide-based RRAM [114].

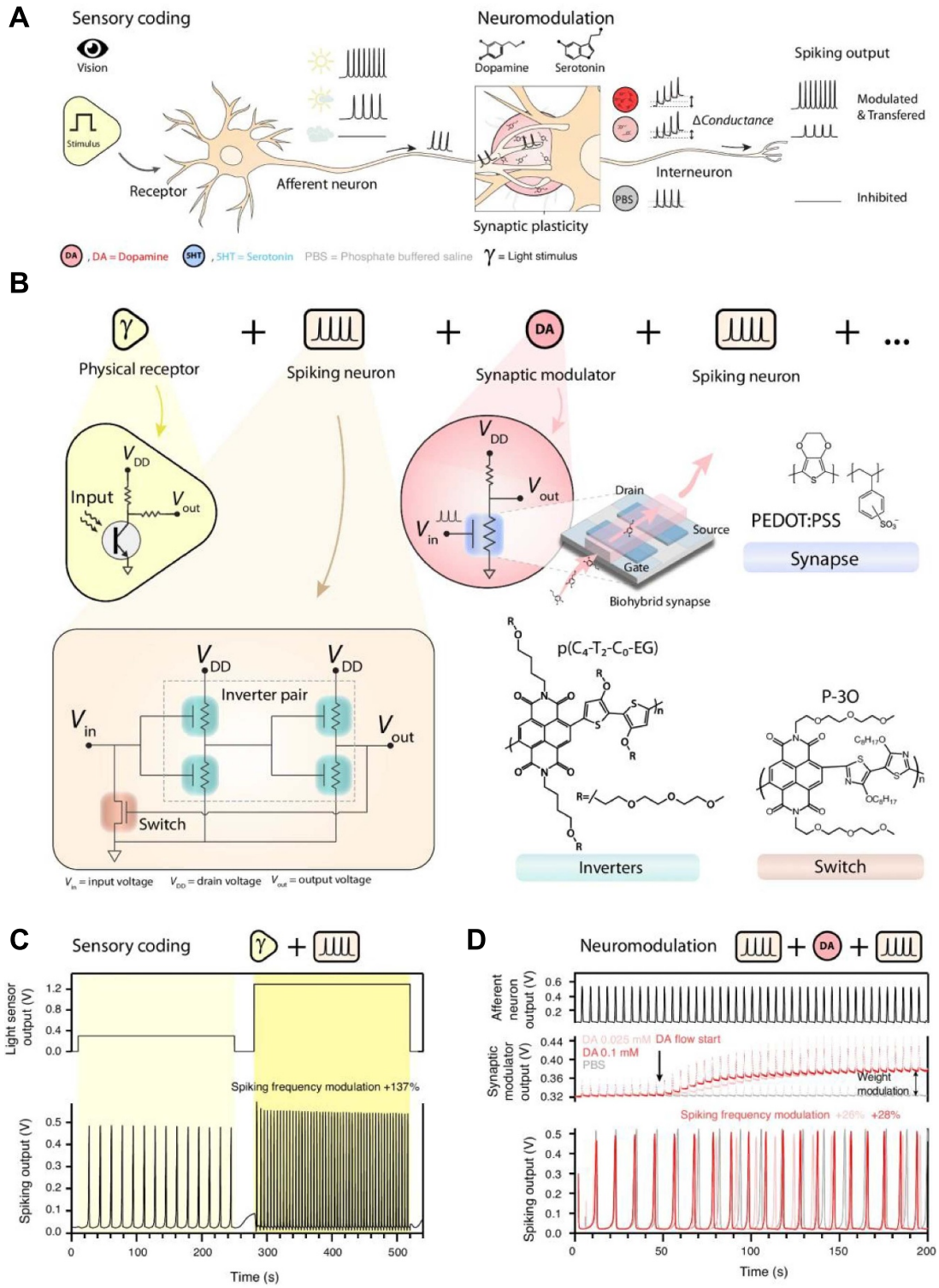

Figure 5. (A) Sensory coding of light stimuli and dopamine regulated neuromodulation of human retina. (B) Schematic of modular neural pathway including a photoreceptor, spiking neuron consisting of inverter pair and a switch, and synaptic modulator comprising a biohybrid synapse using PEDOT:PSS. (C) Sensory coding of light stimulus, showing an increasing spike frequency with increasing light intensity and increasing output voltage of the light sensor. (D) Neuromodulation regulated by dopamine of different concentration. Reproduced from [110]. CC BY 4.0.

For homogeneous configuration, in 2018, the research work by Sun *et al* introduced a photo-synaptic device leveraging indium–gallium–zinc oxide (IGZO) and alkylated graphene oxide (GO) hybrid structures to emulate synaptic functionalities, where GO provides the trapping centres and IGZO acts as charge transporting layer in a transistor configuration [89]. The device demonstrated key synaptic properties, such as excitatory and inhibitory postsynaptic currents (EPSC/IPSC), short-term plasticity (STP), and long-term potentiation/depression (LTP/LTD). By integrating light- and voltage-controlled

weight updating mechanisms, the conductance changes (ΔG) under mixed light and voltage gate spikes increased from 2.32 nS to 5.95 nS compared to voltage-only control. In ANN simulations for MNIST recognition task, the recognition rate improved significantly from 36% to 50% for 20 weight states and from 49% to 62% for 100 weight states, showcasing the device's potential for efficient, low-power neuromorphic applications. Later in 2019, Zhou *et al* presented an optoelectronic RRAM (ORRAM) device designed to emulate retinomorphic vision, integrating sensing, memory, and processing functions within a simple two-terminal structure of Pd/MoO_x/ITO [115]. The device demonstrated UV light-triggered non-volatile resistance switching and tuneable synaptic behaviours, including short-term and long-term plasticity. Through a combination of experimental and theoretical analyses, the authors elucidated the mechanism underlying the low-resistance state (LRS) switching in the ORRAM device. They demonstrated that UV light exposure induces a valence transition of Mo ions from Mo^{6+} to Mo^{5+}, facilitated by the incorporation of protons. This transition shifts the valence band and leads to the formation of a H_yMoO*x* conductive percolation network within the MoO*x* thin film. The device's memory capabilities and nonlinear photoresponsivity enable real-time image processing tasks, including noise reduction and contrast enhancement. Experimentally validated ORRAM arrays demonstrated robust functionalities in image sensing and contrast enhancement, while simulations of ORRAM arrays incorporated into ANNs revealed significantly improved image recognition accuracy and processing efficiency. This work highlights the promising potential of ORRAM devices for neuromorphic visual systems, offering reduced system complexity and fully light-configurable synaptic plasticity (albeit limited to potentiation).

4.3. 2D materials

2D materials are promising candidates for the retinomorphic devices because of their atomic scale thickness, tunable bandgap [116], high carrier mobility [117], immunity to short channel effects [118], excellent light matter interactions [119], mechanical flexibility [120], high transparency, and strong quantum confinement [121]. The operation of a retinomorphic device includes the transformation of optical stimuli into electrical signals by photoconduction, photogating, and photovoltaic effect [122]. 2D materials have the advantage that their persistent photoconductivity (PPC) allows the photocurrent to last even after the light stimulus is removed. The PPC is due to a number of factors, such as defect mediated carrier trapping, phase changes, ion migration and energy barriers that suppress the charge carrier recombination. The device resistance acts as synaptic weight, and by controlling the transport and recombination of photogenerated carriers, the device resistance can be precisely modulated. The charge trapping and de-trapping also has an effect on the photogenerated carriers' transport [122, 123]. The most common 2D materials applied for retinomorphic devices are transition metal dichalcogenides (TMDCs) [124], MXenes [125], group IV elements, such as graphene [126, 127], and group III–V compounds, such as h-BN [37], In_2Se_3 [128] and black phosphorous (BP) [129].

Graphene has a hexagonal honeycomb lattice with single atom layer structure. It is environmentally stable, flexible, optically transparent, and has high carrier mobility [130]. Fu *et al* [126] fabricated graphene/$MoS_{2-x}O_x$/graphene photo-memristor that combines the optical sensing and memory in a single device. The device showed multistate photoresponse with tunable intensity, high endurance over 100 cycles, and state retention for more than 1000 s. It demonstrated image pre-processing (e.g. edge detection, Gaussian blur) using photo-memristor arrays (PMAs) configured with different response states and acted as a classifier by implementing a single-layer perceptron (SLP) to recognise patterns from the MNIST dataset with 96.44% accuracy. Han *et al* [127] also fabricated a WSe_2 phototransistor with graphene as asymmetric electrodes to facilitate charge transport and enhance device functionality. The device generated a bidirectional photocurrent in response to light, regulated by the polarity of the gate voltage. The device emulated the photoreceptor layer (light detection) and bipolar cell layer (ON/OFF signal polarity) of the human retina and reproduced biological visual processes like motion detection and edge enhancement. This research marks a significant step toward low-power artificial visual systems by integration of sensing, memory, and processing into a single device.

2D hexagonal boron nitride (h-BN) also has honeycomb structure like graphene with a wide bandgap of ∼6 eV. h-BN is optically transparent and has low light absorption in the range of 250–900 nm wavelength [131, 132]. h-BN has thickness dependent dielectric properties and its monolayer shows a dielectric constant comparable to SiO_2 with a dangling bond-free surface tolerant to high temperatures [133]. Therefore, in 2D heterogeneous structures for optoelectronic applications, it is mostly used as a gate dielectric to suppress interface scattering and reduce fabrication induced impurities [37].

Black phosphorus shows semiconducting properties due to its puckered honeycomb structure formed by sp^3 hybridised phosphorous atoms [134]. It exhibits p-type semiconducting characteristics and has high carrier mobility. Unlike TMDCs, BP shows direct bandgap characteristics irrespective of thickness

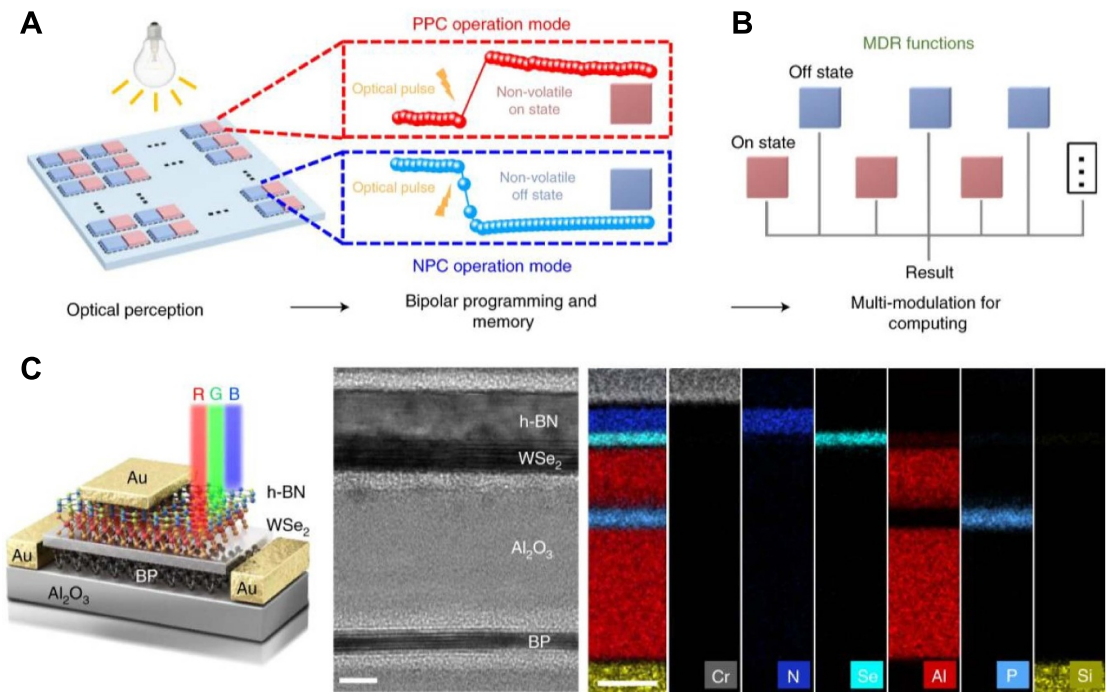

Figure 6. Retina-inspired BP/Al_2O_3/WSe_2/h-BN retinomorphic hardware for motion detection and recognition. (A)–(B) the optical perception and response of the 2D materials replicate the signal collection and conversion of the photoreceptors. The gate pulse-programmable positive and negative non-volatile on/off states mimic the antagonistic shunting and memory of bipolar cells. Also, the laser pulse intensity, number and width modulation mimic the multi-signal regulation abilities of amacrine and ganglion cells to achieve efficient motion detection and recognition (MDR). (C) BP/Al_2O_3/WSe_2/h-BN heterogeneous device structure and scanning transmission electron microscope (STEM) and energy dispersive x-ray spectroscopy (EDS) elemental mapping is shown with scales of 5 nm (left) and 20 nm (right), respectively. Reproduced from [37], with permission from Springer Nature.

[135]. Lee *et al* [129] demonstrated a phototransistor array based on BP for multispectral infrared imaging and in-sensor computing for efficient and adaptive vision in distributed environment. Ahmed *et al* [136] introduced a few-layer BP based optically stimulated artificial synapses for retinotopic applications. By using the oxidation related defects in BP, the device uses 280 nm illumination to induce the excitatory postsynaptic current and a 365 nm illumination to generate IPSC to replicate the light sensitive behaviour of retinal ganglion cells.

TMDCs are layered materials with a general formula MX_2, where M denotes transition metals, such as Mo, W, Pt, Re, and X denotes chalcogen atoms, such as S, Se, and Te. Due to its higher carrier mobility and optical transparency, MoS_2 is widely employed in optoelectronic applications [137–139]. Zhang *et al* [37] presented a motion detection and recognition (MDR) unit using a retina-inspired hardware device based on a 2D BP/Al_2O_3/WSe_2/h-BN heterostructure (figure 6). This device integrated optical perception, memory and computing into a single unit, enabling compact and efficient MDR systems. The device showed progressively tunable positive and negative photoconductivity to replicate the photoreceptors, bipolar cells, amacrine and ganglions in the retina. The device supported MDR with high accuracy and low complexity. Frame difference calculations were used to detect motion efficiently, while the device can perform trichromatic (red, green, blue) motion separation with no ghosting.

Peng *et al* [72] introduced a hardware based artificial vision system that emulates the human vision system which includes the retina and visual cortex. They used 2D WSe_2 to replicate human vision's multifunctional capabilities, such as colour processing. The hardware explained the cause of red–green colour blindness (failure in R–G pathways) and replicates this deficiency in experiments. The hardware demonstrated how the visual pathway detects and processes shape, using double layer sparse neural network with a recognition accuracy above 95%. It implements Barlow Levick model used by humans for direction selective motion tracking in one dimension and two-dimension planes with precise timing. This work has applications in machine vision, autonomous vehicles, brain computer interfaces, and intelligent robotics. The crossbar array of 2D WSe_2 split-floating gate device is used for emulating the retinal and cortical neural functions and the integration of peripheral circuits for connecting retinal functions to cortical level processing. It worked both in photovoltaic mode, which simulates the retina by creating centre-surround receptive fields for light intensity processing, and bipolar transistor mode, which

replicates the neural network of the visual cortex for computations like matrix multiplication. It utilised nearly zero standby power in diode mode and less than one picojoule per operation in transistor mode. Wu *et al* [140] fabricated a biomimetic tetrachromatic photoreceptor using a fully light-controlled WSe_2 p-type transistor, integrating UV–visible light detection, optical synaptic plasticity, and in-sensor processing with lower power consumption.

Wang *et al* [141] presented a 2D mid-infrared optoelectronic retina that simultaneously perceive and encode mid-infrared light stimuli into neural-like spike trains. This retinomorphic system integrates the narrow bandgap and high mid-infrared (MIR) absorption efficiency of black arsenic-phosphorous (b-AsP) and the near-infrared (NIR) sensitivity of $MoTe_2$ 2D van der Waals heterostructures and operates using all optical mechanisms. In perception, the MIR light generates a photocurrent in the b-AsP/$MoTe_2$. While encoding, the NIR pulses modulate these photocurrents. A spike is generated when the current surpasses a threshold, mimicking the spike-based encoding seen in biological systems. In visual adaptation, the retina can handle both the high power and low power MIR targets, and the dynamic range is tuned by changing the mean and variance of the NIR pulse distribution. This demonstrated high MIR detectivity and a fast NIR photo-response time of 600 ns. The SNN achieved excellent accuracy of 96% for image classification tasks, proving the efficiency of the encoded spike data.

Li *et al* [128] developed a 2D ferroelectric field effect transistor (Fe-FET) retinomorphic sensor that combines perception memory and computation for ANNs. Their work addressed the limitations of existing 2D materials by introducing a new gate dielectric $In_2Se_{3-x}O_x$, formed via oxygen plasma treatment, while a few layered $MoSe_2$ is used as the photosensitive channel material. The device exhibits high responsivity (2.4 A W^{-1}), fast response (<20 ms), and achieved 87.9% accuracy in handwritten digit recognition (MNIST dataset). Other commonly used TMDCs for retinomorphic design includes $PtSe_2$ [142], $PtTe_2$ [139], and ReS_2 [143, 144].

MXenes are transition-metal carbides, nitrides, and carbonitrides, derived from MAX phase precursors through selective chemical etching. They are layered structures offering high electrical conductivity and tunable work function by adjusting the surface functional group [145, 146]. Zhao *et al* [125] fabricated a bioinspired photoelectric artificial synaptic transistor using 2D $Ti_3C_2T_x$ MXenes as a floating gate, TiO_2 as tunnelling layer and zinc tin oxide (ZnSnO) as n-type channel material to mimic biological synaptic behaviour for neuromorphic applications. The device responds to UV light stimulation [125].

4.4. Metal halide perovskites

Metal halide perovskite (MHP) materials have been explored as promising candidates for a variety of optoelectronic devices, such as solar cells [147], light-emitting diodes (LEDs) [148], memristors [149] and photodetectors [150]. MHP materials have unique optoelectronic properties, such as long carrier diffusion length [151], low defect density [152], high absorption coefficient [153], high mobility [154], small exciton binding energy [155], and tuneable bandgap [156]. Moreover, owing to the excellent device efficiency and versatile processability (solution deposition) [157, 158], MHPs have established themselves as the next generation of high-performance semiconductors in the past decade.

In contrast to conventional inorganic semiconductors like metal oxides, MHPs exhibit good ionic conductivity derived from their soft lattice and dynamically disordered crystal structure [147, 157]. Slow moving ionic migration has been postulated as the underlying mechanism for anomalous hysteresis behaviour in perovskite solar cells. The ionic conductivity can be detrimental in applications areas, such as photovoltaics [159], LEDs [160], and photodetectors, but such behaviour is promising for machine vision systems [161].

Traditional silicon-based photoelectric sensors, due to their fixed photosensitivity, struggle to deliver high-precision imaging under extreme lighting conditions, such as overly bright or dim environments [162]. To address this limitation, Chen *et al* [163] developed a self-adaptive retinomorphic system based on ternary cation $Cs_{0.05}FA_{0.81}MA_{0.14}PbI_{2.55}Br_{0.45}$ (CsFAMA) lead (Pb) halide perovskite. This system integrates 'sensor-memory-processor' functionalities in a single device and enables optimised imaging quality. Both light exposure and electric bias can tune the device's responsivity, a result of ion migration within the perovskite layer. Furthermore, a multilayer perceptron neural network (PNN) was employed for real-time computational tasks. The perovskite memristor effectively filters background noise, allowing overexposed images of objects like aircraft, vehicles, and birds (which share similar morphological features) to be distinguished with an accuracy improvement of up to 263% after 4.2 s of adaptation time. However, these results, including the device's multiply-accumulate operations and neuromorphic computing capabilities, were obtained through simulations, emphasising the need for experimental verification with real device arrays before practical implementation.

To explore large-scale integration prospects, Zhu *et al* [164] introduced a flexible 32 × 32 sensor array and its functional demonstration in a retinomorphic system. The array consists of phototransistors with a buried-gate structure, where the channel consists of high-purity semiconducting carbon nanotubes (CNTs) and perovskite $CsPbBr_3$ quantum dots (QDs) that act as active materials for electrical transport and photon absorption, respectively. This device combines photodetection and synaptic functions, showcasing both high responsivity and the ability to regulate synaptic plasticity. The array exhibited excellent uniformity and high image sensing quality, mimicking human vision by reinforcing familiar patterns with repeated exposure. Simulations confirmed enhanced learning of facial features with increased training pulses, achieving 95% accuracy after 200 pulses. While reinforcement learning is a key brain-like function, the ability to forget is equally vital. Investigating how electrical/optical pulses can gradually weaken stored signals at the hardware level remains an important area for future research.

Ng *et al* [34] presented a retinomorphic colour perception system, leveraging perovskite bipolar photodetectors to achieve efficient and biologically relevant colour processing. Using a p–i–n–i–p device architecture, employing red–green opponent photodetector (R^+G^-), $FAPbBr_3$ (2.2 eV bandgap) perovskite is used as a green absorber, while $MAPbI_3$ (1.5 eV bandgap) perovskite is employed as a red absorber, as shown in figure 7. These channels replicate the retina's centre-surround antagonistic processing, enabling effective colour differentiation and compression of visual data. This design reduces data transmission requirements by 33% compared to traditional RGB systems, while maintaining minimal loss of colour fidelity. The device's capability extends to high-contrast edge detection and in-sensor convolution by employing interchangeable filters (resembling convolution kernels). The system performs edge detection and sharpening locally, enhancing spatial resolution and object recognition with minimal computational overhead. A significant advancement of this system lies in its adaptive colour perception under varying illumination conditions.

Figure 7(D) illustrates the chromatic cancellation mechanism, where the device adjusts its responsivity to compensate for lighting changes, such as saturation or brightness variations. This adaptation ensures partial colour constancy, which is critical for real-world applications like dynamic visual environments or colour-sensitive tasks in robotics and AI. Another crucial feature of this system is its self-powered operation, enabled by the energy-harvesting properties of perovskites. This eliminates the need for external power sources, making the device scalable and sustainable for widespread deployment. The use of reversible, ion-mediated processes for responsivity adjustments ensures stability and reliability, with minimal degradation over time. By combining data compression, noise filtering, and edge enhancement with adaptive perception, it provides a versatile platform for applications in machine vision, neuromorphic computing, and advanced robotics. This pioneering technology sets a new benchmark in artificial colour vision, bridging the gap between sensing and neural-like processing.

Long *et al* [32] presents a new paradigm for artificial vision by integrating filter-free colour vision, adaptive optics, and neuromorphic pre-processing into a hemispherical bionic eye. Leveraging perovskite nanowires and hybrid nanostructures, the device overcomes longstanding limitations of traditional imaging systems, offering energy-efficient and accurate visual capabilities. At the core of this innovation is the hemispherical retina composed of high-density $CsPbI_3$ perovskite nanowires, integrated with SnO_2/NiO double-shell nanotubes. This unique design replicates photoreceptor functionality, while enabling wavelength-sensitive bidirectional synaptic photoresponses. The $CsPbI_3$ nanowires, with a narrow bandgap (∼1.8 eV), cover the visible spectrum, while the surrounding gate effects in the hybrid structure differentiate between blue and red/green light based on photocurrent polarity and amplitude. This property eliminates the need for conventional colour filters, providing a compact, efficient solution for colour recognition. Additionally, the hemispherical geometry ensures superior optical absorption, and a broader field-of-view (FoV) compared to planar devices. The device incorporates adaptive optical elements, including an artificial crystalline lens and an electronic iris made from liquid crystals. These components dynamically control focal lengths and light intensity, mimicking human eye functionality. Unlike mechanical optics, the liquid crystal-based elements are faster, more compact, and energy-efficient, enhancing the bionic eye's versatility in imaging tasks like depth perception and 3D vision. The adaptive optics, combined with the hemispherical retina, contribute to an impressive FoV of over 140°, surpassing the ∼86° of traditional planar sensors. Under zero-bias conditions, the device generates positive photocurrent under blue light and negative photocurrent under red/green light, distinguishing colours based on polarity and amplitude. When external bias is applied, colour selectivity is enhanced, enabling high-fidelity image reconstruction. Reconstructed images, processed through convolutional neural networks (CNNs), achieve superior classification accuracy compared to conventional monochromatic image sensors. The system demonstrated noise filtering by enhancing contrast between target patterns and noise signals, particularly in images with high Gaussian noise. The CNN-based classification of

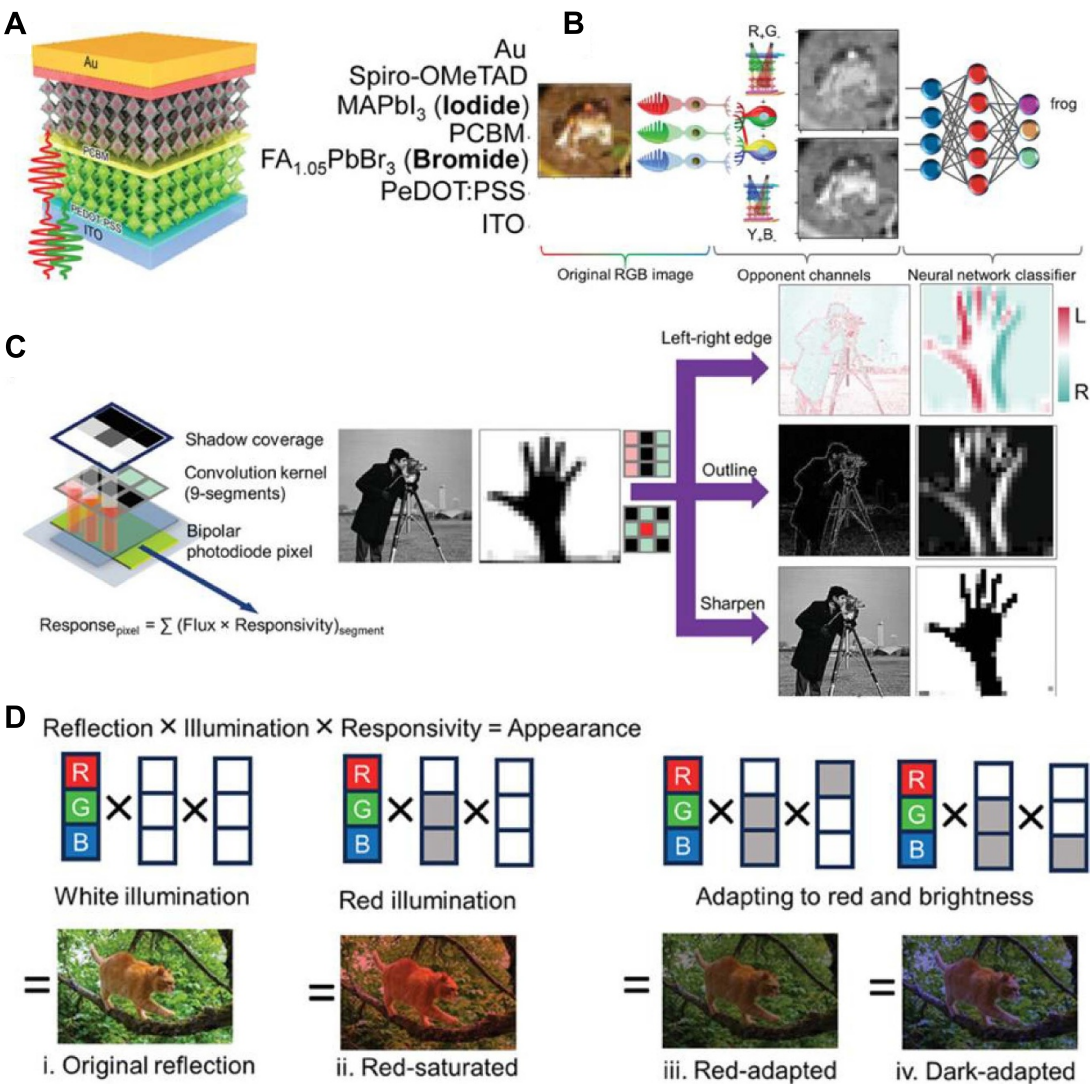

Figure 7. (A) The p–i–n–i–p device configuration consists of ITO/PEDOT:PSS/$FA_{1.05}PbBr_3$/PCBM/$MAPbI_3$/Spiro-OMeTAD/Au. (B) Schematic of colour perception on images from CIFAR10 dataset evaluated by a neural network classifier. (C) In-sensor convolution for high-contrast edge detection. (D) Simulation of red and brightness self-adaptation in the bipolar photodetector-based sensor. [34] John Wiley & Sons. © 2024 Wiley-VCH GmbH.

these processed images achieved 99.4% accuracy, compared to only 11.2% without pre-processing. This highlights the potential of the bionic eye in handling complex visual tasks with enhanced efficiency.

Despite its advancements, challenges remain, such as scaling the device for higher resolution and addressing slower operational speeds under blue light. Nevertheless, this study marks a significant step towards artificial vision systems that emulate biological vision, integrating colour perception, neuromorphic processing, and optical adaptability into a single, compact device.

5. Motion detection with retinomorphic devices

Motion detection has long been recognised as a critical capability for retinomorphic sensors, empowering devices to emulate the advanced functionalities of biological vision systems. The pioneering work of Mead *et al* in the 1980s laid the groundwork for this field by implementing motion detection in retina-inspired devices using CMOS circuitry [1–3, 165]. Conventional image sensors face significant limitations rooted in their architectural design. These sensors capture visual data in discrete frames at fixed intervals, regardless of dynamic changes in the environment. As a result, the temporal quantisation of visual information at predefined frame rates often fails to align with real-time environmental dynamics. Moreover, traditional sensors capture data from all pixels within a frame, even if many pixels record redundant information identical to the previous frame. This redundancy not only constrains temporal

resolution but also imposes substantial demands on data transmission and storage, highlighting the inefficiencies of conventional approaches.

In contrast, biological vision systems demonstrate remarkable efficiency by dynamically responding to events in the visual scene without reliance on fixed intervals or external control signals. The retina processes spatiotemporal information from incident light and converts it into spike trains in particular patterns, which are transmitted to the visual cortex. This highly evolved adaptive filtering and sampling mechanism enhances coding efficiency and minimises data redundancy [21, 22, 166]. Inspired by these biological systems, a frameless, event-driven imaging paradigm for artificial vision has been proposed. This paradigm decentralises control by enabling individual pixels to autonomously capture new information in response to changes in their immediate input. Such event-based designs offer transformative potential for imaging, reducing data redundancy, improving compression, expanding dynamic range, enhancing temporal resolution, and optimising power efficiency [167].

To date, significant research on event cameras has focused on spiking coding and AER communication protocols, first introduced by Boahen in 1996 [8]. Following these foundational developments, numerous designs for event cameras have emerged, exemplified by the widely recognised DVS. Over several generations of iteration, DVS technology has been refined and commercialised in the last decade [168–171]. The DVS responds asynchronously and independently to intensity changes for each pixel, producing a sequence of 'events' or 'spikes'. Each event corresponds to a brightness change at a specific pixel and time, and includes polarity information ('ON' for positive changes, 'OFF' for negative changes), which is transmitted through the AER bus alongside pixel coordinates (x, y) and a timestamp. The bandwidth of the readout circuit is then critical to prevent saturation of the AER bus during high-frequency event emissions, with readout rates ranging from 2 Meps (mega events per second) [172] to 1300 Meps [170]. Event cameras are inherently difference-driven, with output dependence on motion or brightness changes in the scene. Faster motion leads to higher event emission rates, with events timestamped at microsecond resolution and transmitted with sub-millisecond latency [173]. Furthermore, the DVS exhibits high dynamic range and illumination invariance, making it particularly suitable for motion detection. However, its inability to provide absolute intensity measurements and static outputs limits its applicability in some scenarios.

To address these limitations, hybrid designs, such as the asynchronous time-based image sensor (ATIS) [174] and the dynamic and active pixel vision sensor (DVAIS) [172, 175], have been developed. The ATIS integrates a DVS subpixel with an additional subpixel to measure absolute intensity, emitting events that encode the duration required for a predefined threshold of intensity change. Despite its innovation, ATIS suffers from doubled pixel area and inaccuracies in low-light conditions due to extended durations that may be interrupted. Conversely, DVAIS combines a conventional active pixel sensor (APS) with a DVS within the same pixel, sharing a photodiode to measure both intensity changes and absolute values. This hybrid design offers a smaller pixel footprint and operates using both event-driven and frame-based imaging, with APS frames triggered at fixed intervals or in response to DVS events.

The spike-based nature of event cameras requires new paradigms for information extraction and processing. Recent efforts have focused on developing algorithms and hardware implementations to meet these challenges. Event processing typically involves pre-processing at the sensor level, feature extraction and analysis, and post-processing for output. SNNs, convolutional neural networks and graph neural networks have been employed across these stages [176, 177]. Events can be transformed into various representations based on the processing methods, with sophisticated approaches discussed extensively by Gallego *et al* [173].

Event cameras are particularly advantageous for real-time applications, such as robotics, autonomous vehicles, and wearable electronics, where they are used for object tracking, monitoring, and recognition [178]. Additional applications include HDR image reconstruction [179], structured light 3D scanning [180], and optical flow estimation [181]. The asynchronous, low-latency, and high-dynamic-range capabilities of event cameras enable efficient motion detection and tracking. However, event-based algorithms still lag behind frame-based methods in accuracy. Hybrid detectors, combining event- and frame-based modalities, preserve the advantages of both, achieving high-speed tracking (e.g. 5 kHz equivalent frame rates) with bandwidth comparable to conventional 45 fps (frame per second) cameras [35, 182, 183].

Despite these advancements, the pursuit of high-speed vision systems has also explored alternative approaches, such as photonic neural networks [184, 185]. Optical computing methods leverage the inherently high bandwidth and computational speed of photonics, achieving end-to-end latencies in the nanosecond range, while minimising power consumption [186–188].

Most current motion detection systems rely on heterogeneous architectures, where encoding and processing algorithms dominate research efforts. Homogeneous architectures present a promising alternative. One notable possibility is the development of sensors capable of generating spikes like those in event

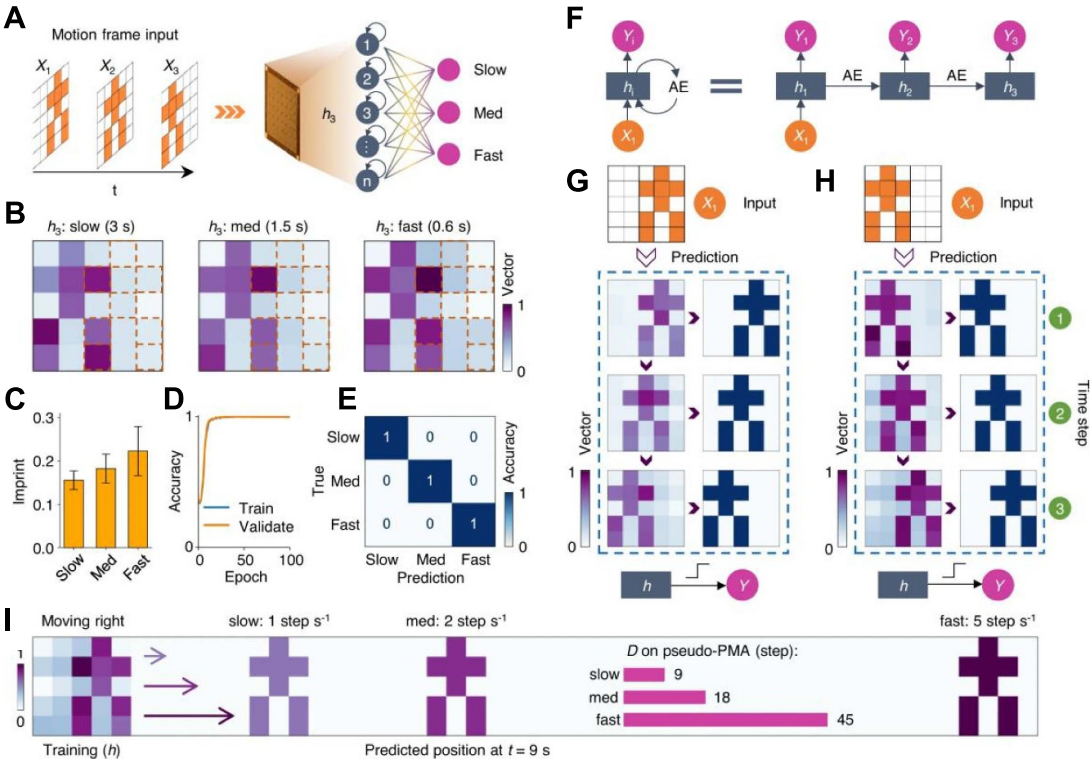

Figure 8. (A) The motion consists of three frames (50 ms illumination per frame) and they are played at three speeds: slow (1 fps), medium (2 fps), and fast (5 fps). (B) The hidden memory states (h_3) of the three motions (slow, medium, fast) were obtained after playing the last frame with $V_{bias} = 1.0$ V. The last frame contains hidden states representing imprints of previous two frames. (C) Portion of imprints from previous frames, calculated by averaging the normalised memory of pixels. High speed results in a stronger imprint because of the rate dependence of hidden memory states. The error bars represent the standard deviation. (D) Training and validation accuracy of the readout network. (E) Confusion matrix of motion speed recognition, showing 100% test accuracy. (F) The system for motion prediction. X_1 indicates the first frame for prediction, AE is the autoencoder network, and Y_i is the predicted output frame. (G)–(H) Prediction of an object moving to the left (G) and the right (H) with input X_1. The predicted output frame of the autoencoder is h. The final output Y is obtained by applying a step function to h. (I) Predicted position and moved distance (D) at $t = 9$ s following the detection of an object moving to the right at three different speeds. Reproduced from [36]. CC BY 4.0.

cameras, but without requiring external circuitry. For instance, vertically stacking photodiode structures, composed of photosensitive materials sandwiched between two metallic layers, function analogously to resistor–capacitor (RC) circuits. These structures exhibit charging and discharging behaviour in response to changes in illumination intensity [77, 189]. However, their output is inherently analogue rather than digital (binary). The spike height represents the rate of change in intensity, making these outputs incompatible with AER protocols without additional analogue-to-digital converter. Nevertheless, the analogue output of these sensors offers a wealth of rich information, making them well-suited for analogue computing approaches, such as reservoir computing [190].

Originally conceived as a framework of recurrent neural networks (RNNs), reservoir computing is particularly proficient at processing temporal and sequential information. The nonlinear dynamic response of such sensors, driven by the evolving states during sensing, positions them as natural candidates for use as reservoirs. Reports have demonstrated their potential for motion detection and prediction, achieving low training costs and high accuracy [36, 191, 192].

For example, Tan and van Dijken [36] developed a machine vision system comprising a 5 × 5 PMA integrated with readout neural networks. This system effectively detected and predicted the motion trajectory of a defined object, underscoring its potential for real-time perception in dynamic machine vision applications. The photo-memristor is a two-terminal device with a structure of ITO/ZnO/Nb-doped $SrTiO_3$ (NSTO), exhibiting dynamic optoelectronic memristive responses characterised by slowly decaying photocurrents after light is turned off. These properties enable the PMA to sense and temporally store optical information. The duration of optical exposure influences the persistence of the imprinted memory, allowing the PMA to embed spatiotemporal information from previous sequential frames as hidden states in the final frame. In their demonstration, three pixelated frames of a moving human figure were projected onto the PMA at varying speeds, 1 fps, 2 fps, and 5 fps, corresponding to 'slow', 'medium', and 'fast' speeds, as shown in figure 8. The data from the final frame were then fed

into a readout neural network designed as a classifier with three outputs. Remarkably, after 100 training epochs, the system achieved near 100% accuracy in speed classification. For motion trajectory prediction, three sequential frames were input into an autoencoder network for training. After training, the system demonstrated the ability to predict future frames using a single input frame. By combining the speed recognition and trajectory prediction networks, the system could accurately forecast the future position of the moving object at different speeds.

6. Challenges and outlook

The concept of retinomorphic devices, which mimic the biological vision system, was introduced nearly half a century ago. In recent years, the development of these devices has witnessed a remarkable surge, driven by the fast-growing interest in developing novel AI hardware technology. Significant innovations have emerged, aiming to address the limitations of conventional machine vision paradigms at the material, device, and integrated system levels. Whilst promising progress has been made, substantial challenges and opportunities remain to be explored.

At materials level, the use of emerging materials, particularly 2D materials and perovskites, has demonstrated notable advantages over conventional silicon in laboratory settings. These materials exhibit unique properties, such as higher photoresponsivity, fast response and tuneable optoelectronic characteristics. However, their reproducibility, long-term stability, and scalability must be addressed to transition from laboratory demonstrations to real-world applications [193–195]. Similarly, while organic materials currently face challenges related to scalability and relatively deficient performance compared to silicon, their potential biocompatibility positions them as promising candidates for biomedical applications, such as retinal prostheses. Metal oxides, on the other hand, present a more promising pathway for large-scale production due to their compatibility with existing CMOS industrial manufacturing technologies. Their success is evidenced by the commercialisation of resistive RAM (RRAM) devices, such as those based on HfOx and NiOx [113, 196], as well as TFTs for flat-panel displays based on IGZO [197, 198]. Table 2 presents a summary of the performance characteristics of retinomorphic devices according to each material class.

At device level, the homogeneous configuration embodies a synergy between photo-sensing and photo-memory. The physical mechanisms underlying the interplay between photo-electron conversion and state switching require further investigation, particularly in the context of emerging materials. Advancing the performance of such devices also hinges on the development of innovative architectures tailored to the distinct physical mechanisms. Drawing inspiration from established designs of memory devices and photodetectors could serve as a valuable strategy. However, a critical challenge lies in the absence of standardised characterisation protocols and benchmarking methodologies for homogeneous retinomorphic devices. For example, energy consumption, a key performance metric, is often inconsistently evaluated. In many cases, reports only consider electric energy consumption during read operations, while excluding the light energy required for write operations or state switching, leading to incomplete assessments [200]. As a subset of neuromorphic hardware, benchmarking frameworks for retinomorphic devices at both the device and system levels could be adapted from methodologies already established for neuromorphic devices [203]. This adaptation not only provides a foundation for performance evaluation but also highlights the critical need for the co-development of retinomorphic devices and their associated external interfaces. The overall performance of a retinomorphic system, encompassing key metrics, such as processing speed and energy consumption, is determined by the integration of the devices and their supporting circuits [10]. Therefore, their design, optimisation, and characterisation must proceed in tandem to ensure a seamless integration and performance improvement. It should be noted that direct comparison of this performance with silicon-based/CMOS devices and systems is not always straightforward, as the latter comprise high density pixel arrays and integration of readout and processing units. Therefore, the figures of merit are defined differently in these heterogeneous systems than monolithic devices in homogeneous configurations. For example, the characterisation of energy consumption needs to consider contribution from peripheral units. Table 3 depicts some examples of the performance of CMOS retinomorphic devices.

At system level, heterogeneous configurations, which integrate imagers with neuromorphic processing units, have achieved significant breakthroughs. This progress has been well exhibited in the launch of retinomorphic SoC chips ‘Speck’ [57], while homogeneous configurations have lagged far behind, with even the scaling up from single devices to functional arrays proving challenging. In many cases, demonstrations of homogeneous device arrays performing neuromorphic computing rely solely on software simulations rather than physical implementations. Another pressing challenge lies in algorithm development. The cooperative development of more energy efficient neural network models, such as SNNs, is

Table 2. Summary of retinomorphic sensors in homogeneous configuration.

Material class	Key material configuration	Spectral response	Light intensity range	Energy consumption[a]	Emulated retinal functions[b]	Retention time	Response time	Adaptation/ switching time[c]	On/off ratio	Ref
Organic	P3HT:PCBM/PVCN/ PVA/PDPP3T:PCBM	UV–Vis	1–10^6 cd m^{-2} (equiv. 1.46–1464 × 10^3 mW cm^2 @555 nm)	0.4 μJ (optical)	Intensity induced sensitivity adaptation		50 ms	2–100 s		[58]
	C_8-BTBT/PMMA/P (VDF-TrFE)	UV	0.2–32 mW cm^{-2}	1.6 μJ (optical)	Edge detection (centre-surround antagonism)	>1000 s	4–53 ms	60 ms	10^5	[82]
	C_8-BTBT/F_{16}CuPc	UV–Vis-NIR	0.3–10 mW cm^{-2}	2.7 μJ (optical)	Intensity dependent synaptic plasticity	>50 s	5 ms	160 ms		[25]
	P3HT:DAE	UV–Vis		1.5 mJ (optical)	Intensity dependent synaptic plasticity	10^7 s	100 ns	5 s	10^5	[61]
	Organic dyes hydrogel/ Bi_2S_3/PEDOT:PSS	Vis	1–3 mW cm^{-2}	250 μJ (optical)	Multi-colour perception channel Bipolarity of bipolar cells	100–2000 s	100 ms	<1 s		[76]
2D	WSe_2/h-BN	UV–Vis-NIR		26–45 fJ (optical)	Edge detection (centre-surround antagonism)	>1000 s	<10 ms	10–150 ms		[37]
	ReS_2	Vis	11–105 mW cm^{-2}	12 fJ (optical)	Intensity dependent synaptic plasticity	1500 s	<100 ms	100 ms		[144]
	MoS_2/WSe_2	Vis-NIR	10–10^6 μW cm^{-2}	0.3–1.1 pJ (optical)	Intensity dependent synaptic plasticity	90 s	<20 ms	20 ms		[199]
	BP	UV–Vis	3–10 mW cm^{-2}	924 pJ (electrical) 3.5 pJ (optical)	Intensity dependent synaptic plasticity		<100 ms	100 ms		[136]
	$Ti_3C_2T_x$	UV		3.75 pJ (electrical) 100 fJ (optical)	Intensity dependent synaptic plasticity	>200 s	<100 ms	100 ms		[125]

(Continued.)

Table 2. (Continued.)

Perovskite	$(MAPbI_3)_{0.75}(FASnI_3)_{0.25}$	UV–Vis-NIR	1–250 mW cm^{-2}	0.6 nJ (electrical) 15 μJ (optical)	Intensity dependent synaptic plasticity	>30 s	1.2 ms	400 ms	10^6	[200]
	$MAPbBr_3$/PCBM/ $MAPbI_3$ $MAPbBr_2Cl$/PCBM/ $MAPbI_3$	UV–Vis-NIR	1–8 mW cm^{-2}	6 mJ (optical)	Multi- colour perception channel Bipolarity of bipolar cells Intensity induced sensitivity adaptation Edge enhancement (centre-surround antagonism)	300 s	10 ms	20 s		[34]
	SnO_2/$CsPbI_3$/NiO	Vis	8–4 × 10^4 μW cm^{-2}	0.2 mJ (optical)	Multi-colour perception channel Bipolarity of bipolar cells Intensity induced sensitivity adaptation Intensity dependent synaptic plasticity	>60 s	<1 s	5–10 s		[32]
	$Cs_{0.05}FA_{0.81}MA_{0.14}$ $PbI_{2.55}Br_{0.45}$	Vis	0.5–256 mW cm^{-2}		Intensity (voltage) induced sensitivity adaptation		<50 ms	50 ms		[163]
	$CsPbBr_3$-QDs	UV–Vis-NIR	10–10^7 nW cm^{-2}	10 nJ (optical)	Intensity induced synaptic plasticity	>200 s	3.3 ms	20 ms		[164]

(Continued.)

Table 2. (Continued.)

Metal Oxide	GO/IGZO	UV	7–140 mW cm^{-2}	160 pJ (electrical) 362 pJ (optical	Intensity induced synaptic plasticity	1000 s	<50 ms	50 ms	[89]
	MoO_x	UV	0.2–200 mW cm^{-2}	500 μJ (optical)	Intensity induced synaptic plasticity	>10^5 s	<200 ms	200 ms	[115]
	$BaTiO_3$	Vis		12 μJ (optical)	Intensity induced synaptic plasticity	>10^4 s		50 s 100 μs (electrical)	[64]
	VO_2	NIR		23.5 pJ (optical)	Intensity induced synaptic plasticity	>600 s	100 ns	150 ms	[201]
	In_2O_3/ZnO	UV	0.4−4 mW cm^{-2}		Intensity induced synaptic plasticity	>30 s	5 ms	100 ms	[202]

[a] If not explicitly addressed as energy consumption per operation, energy consumption is taken as the minimum values of energy that caused noticeable switching of (long-term) synaptic plasticity in the respective article.

[b] This is in addition to the function of photo detection and imaging.

[c] If not explicitly addressed as the switching/adaption time, it refers to the minimum light exposure time that caused noticeable switching of (long-term) synaptic plasticity in the respective article.

Table 3. Examples of retinomorphic devices based on CMOS technology.

	CMOS technology	Pixel array	Dynamic range	Power/energy consumption[a]	Types	Emulated functions	Event rate	Frame rate[b]	References
Silicon	180 nm	240 × 180	130 dB	115 nW/pixel	Event based	Event driven sensing	50 Meps	300 k fps	[172]
	65 nm	1280 × 960		122 nW/pixel	Event based	Event driven sensing	1300 Meps		[170]
	180 nm	64 × 64		35.6 pJ/pixel/frame@510fps 2.1 nJ/block/frame @890fps	Frame based	In-pixel differencing		510 fps 890 fps	[204]
	180 nm	304 × 240	143 dB	680 nW/pixel	Frame based and Event based	Event driven sensing		30–50 k fps	[174]

[a] Silicon-based retinomorphic sensors are developed mostly in a heterogeneous configuration with high-density pixel arrays and integration of readout and processing units. The figures of merit are defined differently than those of monolithic devices in homogeneous configuration. For example, the characterisation of energy consumption needs to consider the contribution from peripheral units.

[b] The equivalent frame rate for event-based sensors is calculated from latency.

essential. These models are inherently better suited to neuromorphic hardware platforms compared to conventional GPUs or CPUs [205–207]. Aligning algorithm design with hardware advancements is critical for unlocking the full potential of retinomorphic devices.

With regard to applications, particularly motion detection and tracking, has emerged as one of the most compelling areas of exploration since the birth of the retinomorphic concept. The dynamic adaptability, low latency, low data demands, and high efficiency of event-based machine vision could provide revolutionary advantages over traditional frame-based machine vision in various applications. This unique capability has not only sparked significant academic interest but also drawn substantial attention from industry. Commercialisation attempts range from vision restoration and industrial monitoring to wearable and mobile devices, autonomous vehicles, and robotics, illustrating the broad scope and versatility of retinomorphic technologies [170, 171, 208, 209]. Beyond serving as bio-inspired replacements or complements to the human eye in retinal prosthetics for vision restoration, retinomorphic devices can provide low-power, real-time visual processing in compact form factors ideally suited for augmented and virtual reality (AR/VR) headsets and smart glasses, where conventional image sensors and processors are limited by latency and energy consumption. In industrial monitoring, their high dynamic range and motion sensitivity can enable fault detection in manufacturing lines, structural health monitoring, and predictive maintenance under challenging lighting or environmental conditions. Looking further ahead in the future, for autonomous vehicles and drones, retinomorphic vision offers faster reaction times to sudden changes in the environment, such as obstacles, pedestrians, or traffic events, which are crucial for safety and navigation. In robotics, these devices can support adaptive, low-latency vision for grasping, locomotion, and human-robot interaction, enabling robots to operate more effectively in unstructured and dynamic environments. Materials enabling lightweight and flexible architectures also make them promising for wearable health monitoring systems, such as eye-tracking, fatigue detection, or gesture recognition in mobile electronics. Finally, the combination of retinomorphic sensors with neuromorphic processors opens opportunities for energy-efficient edge AI, where perception and computation are integrated for smart IoT devices that can interpret complex visual scenes without reliance on cloud-based processing.

In summary, research efforts need to focus on remaining key issues, especially with retinomorphic devices based on organic, perovskite, and 2D materials, relevant to large-scale integration, long-term operational stability, and compatibility with CMOS technologies. Continued interdisciplinary collaboration between materials science, device engineering, the development of novel fabrication techniques, assisted by machine learning, and tailored algorithms through software-hardware co-design will provide a robust foundation for further evolution of this field. Currently, a significant barrier is the absence of a clearly defined functional framework and standardised characterisation protocols, especially for homogeneous device configurations. These are crucial for validating the advantages of retinomorphic devices over conventional silicon-based technologies. Despite these challenges, the outlook for retinomorphic devices for machine vision remains promising. With sustained efforts, they have the potential to revolutionise bio-inspired sensing and computing and open new frontiers in AI, biomedical applications, and beyond.

Data availability statement

All data that support the findings of this study are included within the article (and any supplementary files).

Acknowledgments

All authors wish to acknowledge the support from the UKRI Future Leaders Fellowship Grant (MR/V024442/1). D G G also acknowledges support from European Union's HORIZON Europe Project TEAM-NANO under Grant Agreement No. 101136388 and EPSRC Award: UK Multidisciplinary Centre for Neuromorphic Computing (UKRI982).

Conflict of interest

The authors declare no competing interests.

Author contributions

Yuxin Xia 0000-0002-2566-5645
Writing – original draft (lead), Writing – review & editing (lead)

Roshni Satheesh Babu 0009-0003-8868-6886
Writing – original draft (equal), Writing – review & editing (equal)

Sujaya Kumar Vishwanath 0000-0002-4526-1453
Writing – original draft (equal)

Dimitra G Georgiadou 0000-0002-2620-3346
Conceptualization (lead), Funding acquisition (lead), Supervision (lead), Writing – review & editing (lead)

References

[1] Sivilotti M A, Mahowald M A and Mead C A 1988 *Real-time Visual Computations Using Analog CMOS Processing Arrays* (MIT Press) p 701
[2] Mead C 1989 *Analog VLSI and Neural Systems* (Addison-Wesley) pp 189–21
[3] Mead C 1990 Neuromorphic electronic systems *Proc. IEEE* **78** 1629
[4] Rao A and Akers L A 1990 *1990 IJCNN Int. Joint Conf. on Neural Networks* vol 2 pp 949
[5] Lange E, Funatsu E, Hara K and Kyuma K 1993 *1993 Int. Joint Conf. on Neural Networks* vol 1 pp 801
[6] Nguyen P, Bernard T, Devos F and Zavidovique B 1993 A vision peripheral unit based on a 65x76 smart retina *IFAC Proc. Vol.* **25** 377
[7] Mahowald M A and Mead C 1991 The silicon retina *Sci. Am.* **264** 76
[8] Boahen K A 1996 A retinomorphic vision system *IEEE Micro* **16** 30
[9] Waldrop M M 2016 The chips are down for Moore's law *Nature* **530** 144
[10] Chai Y 2020 In-sensor computing for machine vision *Nature* **579** 32
[11] Chen W, Zhang Z and Liu G 2022 Retinomorphic optoelectronic devices for intelligent machine vision *iScience* **25** 103729
[12] Seok H, Lee D, Son S, Choi H, Kim G and Kim T 2024 Beyond von Neumann architecture: brain-inspired artificial neuromorphic devices and integrated computing *Adv. Electron. Mater.* **10** 2300839
[13] Gregg R G, McCall M A and Massey S C 2013 Function and anatomy of the mammalian retina *Retina* 5th edn (W.B. Saunders) ch 15
[14] Asadi K 2020 Resistance switching in two-terminal ferroelectric-semiconductor lateral heterostructures *Appl. Phys. Rev.* **7** 021307
[15] Cioffi C L 2020 Introduction: overview of the human eye, mammalian retina, and the retinoid visual cycle *Drug Delivery Challenges and Novel Therapeutic Approaches for Retinal Diseases* (Springer) ch 1
[16] Baden T and Nilsson D E 2022 Is our retina really upside down? *Curr. Biol.* **32** R300
[17] Gollisch T and Meister M 2010 Eye smarter than scientists believed: neural computations in circuits of the retina *Neuron* **65** 150
[18] Masland R H 2012 The neuronal organization of the retina *Neuron* **76** 266
[19] Ölveczky B P, Baccus S A and Meister M 2003 Segregation of object and background motion in the retina *Nature* **423** 401
[20] Berry M J, Brivanlou I H, Jordan T A and Meister M 1999 Anticipation of moving stimuli by the retina *Nature* **398** 334
[21] Sterling P 2003 How retinal circuits optimize the transfer of visual information *The Visual Neurosciences* (The MIT Press) ch 17
[22] Zheng Y, Jia S, Yu Z, Liu J K and Huang T 2021 Unraveling neural coding of dynamic natural visual scenes via convolutional recurrent neural networks *Patterns* **2** 100350
[23] Liao F *et al* 2022 Bioinspired in-sensor visual adaptation for accurate perception *Nat. Electron.* **5** 84
[24] Mahabadi N and Khalili Y A 2024 Neuroanatomy, retina (available at: www.ncbi.nlm.nih.gov/books/NBK545310/)
[25] Hao Z *et al* 2022 Retina-inspired self-powered artificial optoelectronic synapses with selective detection in organic asymmetric heterojunctions *Adv. Sci.* **9** e2103494
[26] Kim M S, Yeo J E, Choi H, Chang S H, Kim D H and Song Y M 2023 Evolution of natural eyes and biomimetic imaging devices for effective image acquisition *J. Mater. Chem. C* **11** 12083
[27] Lee G J, Choi C, Kim D-H and Song Y M 2018 Bioinspired artificial eyes: optic components, digital cameras, and visual prostheses *Adv. Funct. Mater.* **28** 201705202
[28] Kim S G, Kim D, Kim S, Yoon J and Lee H S 2019 Human-iris-like aperture and sphincter muscle comprising hyperelastic composite hydrogels containing graphene oxide *Macromol. Mater. Eng.* **304** 1438
[29] Lee G J, Nam W I and Song Y M 2017 Robustness of an artificially tailored fisheye imaging system with a curvilinear image surface *Opt. Laser Technol.* **96** 50
[30] Jang J, Park Y G, Cha E, Ji S, Hwang H, Kim G G, Jin J and Park J U 2021 3D heterogeneous device arrays for multiplexed sensing platforms using transfer of perovskites *Adv. Mater.* **33** 2101093
[31] Gu L *et al* 2020 A biomimetic eye with a hemispherical perovskite nanowire array retina *Nature* **581** 278
[32] Long Z *et al* 2023 A neuromorphic bionic eye with filter-free color vision using hemispherical perovskite nanowire array retina *Nat. Commun.* **14** 1972
[33] Ouyang B, Wang J, Zeng G, Yan J, Zhou Y, Jiang X, Shao B and Chai Y 2024 Bioinspired in-sensor spectral adaptation for perceiving spectrally distinctive features *Nat. Electron.* **7** 705
[34] Ng S E *et al* 2024 Retinomorphic color perception based on opponent process enabled by perovskite bipolar photodetectors *Adv. Mater.* **36** 2406568
[35] Gehrig D and Scaramuzza D 2024 Low-latency automotive vision with event cameras *Nature* **629** 1034
[36] Tan H and van Dijken S 2023 Dynamic machine vision with retinomorphic photomemristor-reservoir computing *Nat. Commun.* **14** 2169
[37] Zhang Z, Wang S, Liu C, Xie R, Hu W and Zhou P 2022 All-in-one two-dimensional retinomorphic hardware device for motion detection and recognition *Nat. Nanotechnol.* **17** 27

[38] Barranco F, Díaz J, Ros E and Del Pino B 2009 Visual system based on artificial retina for motion detection *IEEE Trans. Syst. Man Cybern. B* **39** 752
[39] Yao P *et al* 2017 Face classification using electronic synapses *Nat. Commun.* **8** 15199
[40] Mennel L *et al* 2020 Ultrafast machine vision with 2D material neural network image sensors *Nature* **579** 62
[41] Cai Y *et al* 2023 Broadband visual adaption and image recognition in a monolithic neuromorphic machine vision system *Adv. Funct. Mater.* **33** 2212917
[42] Zhou F and Chai Y 2020 Near-sensor and in-sensor computing *Nat. Electron.* **3** 664
[43] Chen S, Lou Z, Chen D and Shen G 2018 An artificial flexible visual memory system based on an UV-motivated memristor *Adv. Mater.* **30** 1705400
[44] Bi Z, Dong S, Tian Y and Huang T 2018 *Data Compression Conf. Proc.* p 117
[45] Sun L, Wang Z, Jiang J, Kim Y, Joo B, Zheng S, Lee S, Yu W J, Kong B-S and Yang H 2021 In-sensor reservoir computing for language learning via two-dimensional memristors *Sci. Adv.* **7** eabg1455
[46] Yildirim M, Babacan Y and Kacar F 2018 Memristive retinomorphic grid architecture removing noise and preserving edge *AEU-Int. J. Electron. Commun.* **97** 38
[47] Li P *et al* 2024 Reconfigurable optoelectronic transistors for multimodal recognition *Nat. Commun.* **15** 3257
[48] Sivilotti M A 1991 Wiring considerations in analog VLSI systems, with application to field-programmable networks *PhD Thesis*
[49] Zaghloul K A and Boahen K 2006 A silicon retina that reproduces signals in the optic nerve *J. Neural Eng.* **3** 257
[50] Serrano-Gotarredona R *et al* 2009 CAVIAR: a 45k neuron, 5M synapse, 12G connects/s AER hardware sensory-processing-learning-actuating system for high-speed visual object recognition and tracking *IEEE Trans. Neural Netw.* **20** 1417
[51] Mead C and Ismail M 2011 *Analog VLSI Implementation of Neural Systems* (Springer)
[52] Buhmann J M, Lades M and Eeckman F 1993 *Proc. 6th Int. Conf. on Neural Information Processing Systems* p 769
[53] Neumann J V 1993 First draft of a report on the EDVAC | IEEE Journals & Magazine | IEEE Xplore *IEEE Ann. Hist. Comput.* **15** 14596
[54] Mukhopadhyay S *et al* 2019 Heterogeneous integration for artificial intelligence: challenges and opportunities *IBM J. Res. Dev.* **63** 1
[55] Zhong F M, Chen Z K, Ning Z L, Min G Y and Hu Y M 2018 Heterogeneous visual features integration for image recognition optimization in internet of things *J. Comput. Sci.* **28** 466
[56] Seo S *et al* 2018 Artificial optic-neural synapse for colored and color-mixed pattern recognition *Nat. Commun.* **9** 5106
[57] Yao M *et al* 2024 Spike-based dynamic computing with asynchronous sensing-computing neuromorphic chip *Nat. Commun.* **15** 4464
[58] He Z H, Shen H G, Ye D K, Xiang L Y, Zhao W R, Ding J M, Zhang F J, Di C A and Zhu D B 2021 An organic transistor with light intensity-dependent active photoadaptation *Nat. Electron.* **4** 522
[59] Yildirim M and Kacar F 2020 Retina-inspired neuromorphic edge enhancing and edge detection *AEU- Int. J. Electron. Commun.* **115** 153038
[60] Trujillo Herrera C and Labram J G 2022 An organic retinomorphic sensor *ACS Appl. Electron. Mater.* **4** 92
[61] Leydecker T, Herder M, Pavlica E, Bratina G, Hecht S, Orgiu E and Samorì P 2016 Flexible non-volatile optical memory thin-film transistor device with over 256 distinct levels based on an organic bicomponent blend *Nat. Nanotechnol.* **11** 769
[62] Frohman-Bentchkowsky D 1971 Memory behavior in a floating-gate avalanche-injection MOS (FAMOS) structure *Appl. Phys. Lett.* **18** 332
[63] Orgiu E *et al* 2012 Optically switchable transistor via energy-level phototuning in a bicomponent organic semiconductor *Nat. Chem.* **4** 675
[64] Long X, Tan H, Sanchez F, Fina I and Fontcuberta J 2021 Non-volatile optical switch of resistance in photoferroelectric tunnel junctions *Nat. Commun.* **12** 382
[65] Hosseini P, Wright C D and Bhaskaran H 2014 An optoelectronic framework enabled by low-dimensional phase-change films *Nature* **511** 206
[66] Boybat I, Gallo M L, Nandakumar S R, Moraitis T, Parnell T, Tuma T, Rajendran B, Leblebici Y, Sebastian A and Eleftheriou E 2018 Neuromorphic computing with multi-memristive synapses *Nat. Commun.* **9** 2514
[67] Zhang Y *et al* 2021 Electrically reconfigurable non-volatile metasurface using low-loss optical phase-change material *Nat. Nanotechnol.* **16** 661
[68] Yoon S M, Yang S, Byun C, Park S H K, Cho D H, Jung S W, Kwon O S and Hwang C S 2010 Fully transparent non-volatile memory thin-film transistors using an organic ferroelectric and oxide semiconductor below 200 °C *Adv. Funct. Mater.* **20** 921
[69] Li T *et al* 2018 Optical control of polarization in ferroelectric heterostructures *Nat. Commun.* **9** 3344
[70] Li L, Dai Q, Li Y, Pei M, Osada M and Li Y 2024 Autonomous light intensity adaptation in an energy-efficient retinomorphic organic ferroelectric neuristor *Adv. Opt. Mater.* **12** 2303172
[71] Nur R *et al* 2022 A floating gate negative capacitance MoS_2 phototransistor with high photosensitivity *Nanoscale* **14** 2013
[72] Peng Z *et al* 2024 Multifunctional human visual pathway-replicated hardware based on 2D materials *Nat. Commun.* **15** 8650
[73] Liu Q, Yue W, Li Y, Wang W, Xu L, Wang Y, Gao S, Zhang C, Kan H and Li C 2021 Multifunctional optoelectronic random access memory device based on surface-plasma-treated inorganic halide perovskite *Adv. Electron. Mater.* **7** 2100366
[74] Corrado F *et al* 2023 Azobenzene-based optoelectronic transistors for neurohybrid building blocks *Nat. Commun.* **14** 6760
[75] Chen K *et al* 2023 Organic optoelectronic synapse based on photon-modulated electrochemical doping *Nat. Photon.* **17** 629
[76] Hu J *et al* 2024 A photoelectrochemical retinomorphic synapse *Adv. Mater.* **36** 2405887
[77] Wu S E, Zeng L, Zhai Y, Shin C, Eedugurala N, Azoulay J D and Ng T N 2023 Retinomorphic motion detector fabricated with organic infrared semiconductors *Adv. Sci.* **10** e2304688
[78] Sarwat S G, Kersting B, Moraitis T, Jonnalagadda V P, Sebastian A, Sarwat S G, Kersting B, Moraitis T, Jonnalagadda V P and Sebastian A 2022 Phase-change memtransistive synapses for mixed-plasticity neural computations *Nat. Nanotechnol.* **17** 507
[79] Prabhathan P *et al* 2023 Roadmap for phase change materials in photonics and beyond *iScience* **26** 107946
[80] Loke D, Lee T H, Wang W J, Shi L P, Zhao R, Yeo Y C, Chong T C and Elliott S R 2012 Breaking the speed limits of phase-change memory *Science* **336** 1566
[81] Di Martino G and Tappertzhofen S 2019 Optically accessible memristive devices *Nanophotonics* **8** 1579
[82] Dai Q *et al* 2023 Integration of image preprocessing and recognition functions in an optoelectronic coupling organic ferroelectric retinomorphic neuristor *Mater. Horiz.* **10** 3061
[83] Tsujioka T and Irie M 2010 Electrical functions of photochromic molecules *J. Photochem. Photobiol. C* **11** 1

[84] Zhou X et al 2024 All-photonic artificial synapses based on photochromic perovskites for noncontact neuromorphic visual perception Commun. Mater. 5 116
[85] Yu S H, Hassan S Z, So C, Kang M and Chung D S 2023 Molecular-switch-embedded solution-processed semiconductors Adv. Mater. 35 e2203401
[86] Li D, Zheng X, He H, Boutinaud P, Xiao S, Xu J, Wang C, Hu Y and Kang F 2024 A 20-year review of inorganic photochromic materials: design consideration, synthesis methods, classifications, optical properties, mechanism models, and emerging applications Laser Photon. Rev. 18 2400742
[87] Wu D, Cui X, El-Khouly M E, Gu M, Zhang B and Chen Y 2023 Covalent functionalization of black phosphorus nanosheets with photochromic polymer for transient optoelectronic memory devices Adv. Electron. Mater. 9 2200925
[88] Zhang T, Fan C, Hu L, Zhuge F, Pan X and Ye Z 2024 A reconfigurable all-optical-controlled synaptic device for neuromorphic computing applications ACS Nano 18 16236
[89] Sun J, Oh S, Choi Y, Seo S, Oh M J, Lee M, Lee W B, Yoo P J, Cho J H and Park J-H 2018 Optoelectronic synapse based on IGZO-alkylated graphene oxide hybrid structure Adv. Funct. Mater. 28 1804397
[90] Zhuang Y, Ren X, Che X, Liu S, Huang W and Zhao Q 2020 Organic photoresponsive materials for information storage: a review Adv. Photon. 3 014001
[91] Someya T, Bao Z and Malliaras G G 2016 The rise of plastic bioelectronics Nature 540 379
[92] Chortos A, Liu J and Bao Z 2016 Pursuing prosthetic electronic skin Nat. Mater. 15 937
[93] van de Burgt Y, Melianas A, Keene S T, Malliaras G, Salleo A, van de Burgt Y, Melianas A, Keene S T, Malliaras G and Salleo A 2018 Organic electronics for neuromorphic computing Nat. Electron. 1 386
[94] Nougaret L et al 2014 Nanoscale design of multifunctional organic layers for low-power high-density memory devices ACS Nano 8 3498
[95] Kim Y et al 2018 A bioinspired flexible organic artificial afferent nerve Science 360 998
[96] Ni Y, Liu J, Han H, Yu Q, Yang L, Xu Z, Jiang C, Liu L and Xu W 2024 Visualized in-sensor computing Nat. Commun. 15 3454
[97] Prime D and Paul S 2009 Overview of organic memory devices Phil. Trans. R. Soc. A 367 4141
[98] Hogarth C A and Zor M 1975 Some observations of voltage-induced conductance changes in thin films of evaporated polyethylene Thin Solid Films 27 L5
[99] Hogarth C A and Iqbal T 1979 The electroforming of thin films of polypropylene Int. J. Electron. 47 349
[100] Thurstans R E and Oxley D P 2002 The electroformed metal-insulator-metal structure: a comprehensive model J. Phys. D: Appl. Phys. 35 802
[101] Andersson P, Robinson N D and Berggren M 2005 Switchable charge traps in polymer diodes Adv. Mater. 17 1798
[102] Mo X L, Chen G R, Cai Q J, Fan Z Y, Xu H H, Yao Y, Yang J, Gu H H and Hua Z Y 2003 Preparation and electrical/optical bistable property of potassium tetracyanoquinodimethane thin films Thin Solid Films 436 259
[103] Li Y F 2012 Molecular design of photovoltaic materials for polymer solar cells: toward suitable electronic energy levels and broad absorption Acc. Chem. Res. 45 723
[104] Lu G, Usta H, Risko C, Wang L, Facchetti A, Ratner M A and Marks T J 2008 Synthesis, characterization, and transistor response of semiconducting silole polymers with substantial hole mobility and air stability. Experiment and theory J. Am. Chem. Soc. 130 7670
[105] Kim Y et al 2006 A strong regioregularity effect in self-organizing conjugated polymer films and high-efficiency polythiophene: fullerene solar cells Nat. Mater. 5 197
[106] Shao H et al 2024 Retinomorphic photonic synapses for mimicking ultraviolet radiation sensing and damage imaging Adv. Funct. Mater. 34 202316381
[107] Lan S Q, Zhong J F, Li E L, Yan Y J, Wu X M, Chen Q Z, Lin W K, Chen H P and Guo T L 2020 High-performance nonvolatile organic photoelectronic transistor memory based on bulk heterojunction structure ACS Appl. Mater. Interfaces 12 31716
[108] Lee W Y, Wu H C, Lu C, Naab B D, Chen W C and Bao Z N 2017 n-Type doped conjugated polymer for nonvolatile memory Adv. Mater. 29 201605166
[109] Baeg K J, Noh Y Y, Sirringhaus H and Kim D Y 2010 Controllable shifts in threshold voltage of top-gate polymer field-effect transistors for applications in organic nano floating gate memory Adv. Funct. Mater. 20 224
[110] Matrone G M, van Doremaele E R W, Surendran A, Laswick Z, Griggs S, Ye G, McCulloch I, Santoro F, Rivnay J and van de Burgt Y 2024 A modular organic neuromorphic spiking circuit for retina-inspired sensory coding and neurotransmitter-mediated neural pathways Nat. Commun. 15 2868
[111] Stengel M, Vanderbilt D, Spaldin N A, Stengel M, Vanderbilt D and Spaldin N A 2009 Enhancement of ferroelectricity at metal–oxide interfaces Nat. Mater. 8 392
[112] Kumar D, Aluguri R, Chand U and Tseng T Y 2017 Metal oxide resistive switching memory: materials, properties and switching mechanisms Ceram. Int. 43 S547
[113] Baek I G et al 2004 IEEE Int. Electron Devices Meeting p 587
[114] Prezioso M, Merrikh-Bayat F, Hoskins B D, Adam G C, Likharev K K and Strukov D B 2015 Training and operation of an integrated neuromorphic network based on metal-oxide memristors Nature 521 61
[115] Zhou F et al 2019 Optoelectronic resistive random access memory for neuromorphic vision sensors Nat. Nanotechnol. 14 776
[116] Susarla S, Kutana A, Hachtel J A, Kochat V, Apte A, Vajtai R, Idrobo J C, Yakobson B I, Tiwary C S and Ajayan P M 2017 Quaternary 2D transition metal dichalcogenides (TMDs) with tunable bandgap Adv. Mater. 29 1702457
[117] Bonell F, Marty A, Vergnaud C, Consonni V, Okuno H, Ouerghi A, Boukari H and Jamet M 2021 High carrier mobility in single-crystal PtSe2 grown by molecular beam epitaxy on ZnO (0001) 2D Mater. 9 015015
[118] Xu K, Zhang Z, Wang Z, Wang F, Huang Y, Liao L and He J 2015 Short channel field-effect transistors from ultrathin GaTe nanosheets Appl. Phys. Lett. 107 153507
[119] Huang L, Krasnok A, Alú A, Yu Y, Neshev D and Miroshnichenko A E 2022 Enhanced light–matter interaction in two-dimensional transition metal dichalcogenides Rep. Prog. Phys. 85 046401
[120] Piacentini A, Daus A, Wang Z, Lemme M C and Neumaier D 2023 Potential of transition metal dichalcogenide transistors for flexible electronics applications Adv. Electron. Mater. 9 2300181
[121] Jia G Y, Liu Y, Gong J Y, Lei D Y, Wang D L and Huang Z X 2016 Excitonic quantum confinement modified optical conductivity of monolayer and few-layered MoS_2 J. Mater. Chem. C 4 8822
[122] Jana R, Ghosh S, Bhunia R and Chowdhury A 2024 Recent developments in the state-of-the-art optoelectronic synaptic devices premised on 2D materials: a review J. Mater. Chem. C 12 5299

[123] Zhang Z R, Yang D L, Li H H, Li C, Wang Z R, Sun L F and Yang H J 2022 2D materials and van der Waals heterojunctions for neuromorphic computing *Neuromorph. Comput. Eng.* **2** 032004
[124] Babu R S and Georgiadou D G 2025 2D transition metal dichalcogenides for energy-efficient two-terminal optoelectronic synaptic devices *Device* **3** 100805
[125] Zhao T, Zhao C, Xu W, Liu Y, Gao H, Mitrovic I Z, Lim E G, Yang L and Zhao C Z 2021 Bio-inspired photoelectric artificial synapse based on two-dimensional Ti_3C_2T MXenes floating gate *Adv. Funct. Mater.* **31** 2106000
[126] Fu X, Li T, Cai B, Miao J, Panin G N, Ma X, Wang J, Jiang X, Li Q and Dong Y 2023 Graphene/$MoS_{2-x}O_x$/graphene photomemristor with tunable non-volatile responsivities for neuromorphic vision processing *Light Sci. Appl.* **12** 39
[127] Han Z, Zhang Y, Mi Q, You J, Zhang N, Zhong Z, Jiang Z, Guo H, Hu H and Wang L 2024 Reconfigurable homojunction phototransistor for near-zero power consumption artificial biomimetic retina function *ACS Nano* **18** 29968
[128] Li X, Chen X, Deng W, Li S, An B, Chu F, Wu Y, Liu F and Zhang Y 2023 An all-two-dimensional Fe-FET retinomorphic sensor based on the novel gate dielectric $In_2Se_{3-x}O_x$ *Nanoscale* **15** 10705
[129] Lee S, Peng R, Wu C and Li M 2022 Programmable black phosphorus image sensor for broadband optoelectronic edge computing *Nat. Commun.* **13** 1485
[130] Bonaccorso F, Sun Z, Hasan T and Ferrari A C 2010 Graphene photonics and optoelectronics *Nat. Photon.* **4** 611
[131] Roy S, Zhang X, Puthirath A B, Meiyazhagan A, Bhattacharyya S, Rahman M M, Babu G, Susarla S, Saju S K and Tran M K 2021 Structure, properties and applications of two-dimensional hexagonal boron nitride *Adv. Mater.* **33** 2101589
[132] Zhang L, Dong J and Ding F 2021 Strategies, status, and challenges in wafer scale single crystalline two-dimensional materials synthesis *Chem. Rev.* **121** 6321
[133] Liu Y, Duan X, Huang Y and Duan X 2018 Two-dimensional transistors beyond graphene and TMDCs *Chem. Soc. Rev.* **47** 6388
[134] Zeng Y and Guo Z 2021 Synthesis and stabilization of black phosphorus and phosphorene: recent progress and perspectives *Iscience* **24** 103116
[135] Akinwande D, Huyghebaert C, Wang C H, Serna M I, Goossens S, Li L J, Wong H P and Koppens F H L 2019 Graphene and two-dimensional materials for silicon technology *Nature* **573** 507
[136] Ahmed T, Kuriakose S, Mayes E L H, Ramanathan R, Bansal V, Bhaskaran M, Sriram S and Walia S 2019 Optically stimulated artificial synapse based on layered black phosphorus *Small* **15** 1900966
[137] Singh A K, Kumar P, Late D J, Kumar A, Patel S and Singh J 2018 2D layered transition metal dichalcogenides (MoS_2): synthesis, applications and theoretical aspects *Appl. Mater. Today* **13** 242
[138] Guo P, Jia M, Guo D, Wang Z L and Zhai J 2023 Retina-inspired in-sensor broadband image preprocessing for accurate recognition via the flexophototronic effect *Matter* **6** 537
[139] Shi L, Shi K, Zhang Z C, Li Y, Wang F D, Si S H, Liu Z B, Lu T B, Chen X D and Zhang J 2024 Flexible retinomorphic vision sensors with scotopic and photopic adaptation for a fully flexible neuromorphic machine vision system *Smartmat* **5** e1285
[140] Wu R Q, Liu X C, Yuan Y H, Wang Z W, Jing Y M and Sun J 2023 Biomimetic artificial tetrachromatic photoreceptors based on fully light-controlled 2D transistors *Adv. Funct. Mater.* **33** 202305677
[141] Wang F, Hu F, Dai M, Zhu S, Sun F, Duan R, Wang C, Han J, Deng W and Chen W 2023 A two-dimensional mid-infrared optoelectronic retina enabling simultaneous perception and encoding *Nat. Commun.* **14** 1938
[142] Tan Y, Hao H, Chen Y, Kang Y, Xu T, Li C, Xie X and Jiang T 2022 A bioinspired retinomorphic device for spontaneous chromatic adaptation *Adv. Mater.* **34** 2206816
[143] Guo T, Li S, Zhou Y N, Lu W D, Yan Y and Wu Y A 2024 Interspecies-chimera machine vision with polarimetry for real-time navigation and anti-glare pattern recognition *Nat. Commun.* **15** 6731
[144] Chen Y B, Huang Y J, Zeng J W, Kang Y, Tan Y L, Xie X N, Wei B, Li C, Fang L and Jiang T 2023 Energy-efficient ReS-based optoelectronic synapse for 3D object reconstruction and recognition *ACS Appl. Mater. Interfaces* **15** 58631
[145] Li X, Huang Z, Shuck C E, Liang G, Gogotsi Y and Zhi C 2022 MXene chemistry, electrochemistry and energy storage applications *Nat. Rev. Chem.* **6** 389
[146] Tan H, Tao Q, Pande I, Majumdar S, Liu F, Zhou Y, Persson P O Å, Rosen J and van Dijken S 2020 Tactile sensory coding and learning with bio-inspired optoelectronic spiking afferent nerves *Nat. Commun.* **11** 1369
[147] Lee J-W, Kim S-G, Yang J-M, Yang Y and Park N-G 2019 Verification and mitigation of ion migration in perovskite solar cells *APL Mater.* **7** 041111
[148] Veldhuis S A, Boix P P, Yantara N, Li M, Sum T C, Mathews N and Mhaisalkar S G 2016 Perovskite materials for light-emitting diodes and lasers *Adv. Mater.* **28** 6804
[149] Vishwanath S K *et al* 2024 High-performance one-dimensional halide perovskite crossbar memristors and synapses for neuromorphic computing *Mater. Horiz.* **11** 2643
[150] Georgiadou D G, Lin Y-H, Lim J, Ratnasingham S, McLachlan M A, Snaith H J and Anthopoulos T D 2019 High responsivity and response speed single-layer mixed-cation lead mixed-halide perovskite photodetectors based on nanogap electrodes manufactured on large-area rigid and flexible substrates *Adv. Funct. Mater.* **29** 1901371
[151] Xing G, Mathews N, Sun S, Lim S S, Lam Y M, Grätzel M, Mhaisalkar S and Sum T C 2013 Long-range balanced electron-and hole-transport lengths in organic-inorganic $CH_3NH_3PbI_3$ *Science* **342** 344
[152] Luo D, Yang W, Wang Z, Sadhanala A, Hu Q, Su R, Shivanna R, Trindade G F, Watts J F and Xu Z 2018 Enhanced photovoltage for inverted planar heterojunction perovskite solar cells *Science* **360** 1442
[153] Saouma F O, Park D Y, Kim S H, Jeong M S and Jang J I 2017 Multiphoton absorption coefficients of organic–inorganic lead halide perovskites $CH_3NH_3PbX_3$ (X = Cl, Br, I) single crystals *Chem. Mater.* **29** 6876
[154] Tailor N K, Ranjan R, Ranjan S, Sharma T, Singh A, Garg A, Nalwa K S, Gupta R K and Satapathi S 2021 The effect of dimensionality on the charge carrier mobility of halide perovskites *J. Mater. Chem. A* **9** 21551
[155] Miyata A, Mitioglu A, Plochocka P, Portugall O, Wang J T-W, Stranks S D, Snaith H J and Nicholas R J 2015 Direct measurement of the exciton binding energy and effective masses for charge carriers in organic–inorganic tri-halide perovskites *Nat. Phys.* **11** 582
[156] Unger E, Kegelmann L, Suchan K, Sörell D, Korte L and Albrecht S 2017 Roadmap and roadblocks for the band gap tunability of metal halide perovskites *J. Mater. Chem. A* **5** 11401
[157] Yantara N and Mathews N 2024 Toolsets for assessing ionic migration in halide perovskites *Joule* **8** 1239
[158] Xing G, Mathews N, Lim S S, Yantara N, Liu X, Sabba D, Grätzel M, Mhaisalkar S and Sum T C 2014 Low-temperature solution-processed wavelength-tunable perovskites for lasing *Nat. Mater.* **13** 476
[159] Calado P, Telford A M, Bryant D, Li X, Nelson J, O'regan B C and Barnes P R 2016 Evidence for ion migration in hybrid perovskite solar cells with minimal hysteresis *Nat. Commun.* **7** 13831

[160] Li N, Jia Y, Guo Y and Zhao N 2022 Ion migration in perovskite light-emitting diodes: mechanism, characterizations, and material and device engineering *Adv. Mater.* **34** 2108102
[161] Sharma D, Luqman A, Ng S E, Yantara N, Xing X, Tay Y B, Basu A, Chattopadhyay A and Mathews N 2024 Halide perovskite photovoltaics for in-sensor reservoir computing *Nano Energy* **129** 109949
[162] Fossum E R and Hondongwa D B 2014 A review of the pinned photodiode for CCD and CMOS image sensors *IEEE J. Electron Devices Soc.* **2** 33
[163] Chen Q, Zhang Y, Liu S, Han T, Chen X, Xu Y, Meng Z, Zhang G, Zheng X and Zhao J 2020 Switchable perovskite photovoltaic sensors for bioinspired adaptive machine vision *Adv. Intell. Syst.* **2** 2000122
[164] Zhu Q-B, Li B, Yang D-D, Liu C, Feng S, Chen M-L, Sun Y, Tian Y-N, Su X and Wang X-M 2021 A flexible ultrasensitive optoelectronic sensor array for neuromorphic vision systems *Nat. Commun.* **12** 1798
[165] Hutchinson J, Koch C, Luo J and Mead C 1988 Computing motion using analog and binary resistive networks *Computer* **21** 52
[166] Gollisch T and Meister M 2008 Rapid neural coding in the retina with relative spike latencies *Science* **319** 1108
[167] Posch C, Serrano-Gotarredona T, Linares-Barranco B and Delbruck T 2014 Retinomorphic event-based vision sensors: bioinspired cameras with spiking output *Proc. IEEE* **102** 1470
[168] Lichtsteiner P, Posch C and Delbruck T 2006 *IEEE Int. Solid State Circuits Conf.—Digest of Technical Papers* p 2060
[169] Lichtsteiner P and Delbruck T 2005 *Research in Microelectronics and Electronics* pp 406
[170] Suh Y *et al* 2020 *IEEE Int. Symp. on Circuits and Systems (ISCAS)* p 1
[171] 2024 IniVation products (available at: https://inivation.com/technology/)
[172] Brandli C, Berner R, Minhao Y, Shih-Chii L and Delbruck T 2014 A 240 × 180 130 dB 3 μs latency global shutter spatiotemporal vision sensor *IEEE J. Solid-State Circuits* **49** 2333
[173] Gallego G *et al* 2022 Event-based vision: a survey *IEEE Trans. Pattern Anal.* **44** 154
[174] Posch C, Matolin D and Wohlgenannt R 2011 A QVGA 143 dB dynamic range frame-free PWM image sensor with lossless pixel-level video compression and time-domain CDS *IEEE J. Solid-State Circuits* **46** 259
[175] Berner R, Brandli C, Yang M, Liu S-C and Delbruck T 2013 *IEEE Symp. on VLSI Circuits* pp C186
[176] Yu Q, Tang H, Tan K C and Li H 2013 Precise-spike-driven synaptic plasticity: learning hetero-association of spatiotemporal spike patterns *PLoS One* **8** e78318
[177] Ning L M, Dong J F, Xiao R, Tan K C and Tang H J 2023 Event-driven spiking neural networks with spike-based learning *Memetic Comput.* **15** 205
[178] Delbruck T 2016 *46th European Solid-State Device Research Conf. (Essderc)* (*Lausanne, Switzerland*) p 7
[179] 2024 Akida 2nd generation (available at: https://brainchip.com/akida-generations/)
[180] Matsuda N, Cossairt O and Gupta M 2015 *2015 IEEE International Conference on Computational Photography (ICCP)* p 1
[181] Zhu A Z, Yuan L, Chaney K and Daniilidis K 2018 EV-FlowNet: self-supervised optical flow estimation for event-based cameras (arXiv:1802.06898)
[182] Lele A S, Fang Y, Anwar A and Raychowdhury A 2022 Bio-mimetic high-speed target localization with fused frame and event vision for edge application *Front. Neurosci.* **16** 1010302
[183] Yang Z *et al* 2024 A vision chip with complementary pathways for open-world sensing *Nature* **629** 1027
[184] Stark P, Horst F, Dangel R, Weiss J and Offrein B J 2020 Opportunities for integrated photonic neural networks *Nanophotonics* **9** 4221
[185] Xu X *et al* 2021 11 TOPS photonic convolutional accelerator for optical neural networks *Nature* **589** 44
[186] Xu Z, Yuan X, Zhou T, Fang L, Xu Z, Yuan X, Zhou T and Fang L 2022 A multichannel optical computing architecture for advanced machine vision *Light Sci. Appl.* **11** 255
[187] Chen Y *et al* 2023 All-analog photoelectronic chip for high-speed vision tasks *Nature* **623** 48
[188] Ashtiani F, Geers A J, Aflatouni F, Ashtiani F, Geers A J and Aflatouni F 2022 An on-chip photonic deep neural network for image classification *Nature* **606** 501
[189] Herrera T C and Labram J G 2020 A perovskite retinomorphic sensor *Appl. Phys. Lett.* **117** 233501
[190] Jang Y H, Han J-K, Moon S, Shim S K, Han J, Cheong S, Lee S H and Hwang C S 2024 A high-dimensional in-sensor reservoir computing system with optoelectronic memristors for high-performance neuromorphic machine vision *Mater. Horiz.* **11** 499
[191] Zhong Y, Tang J, Li X, Gao B, Qian H and Wu H 2021 Dynamic memristor-based reservoir computing for high-efficiency temporal signal processing *Nat. Commun.* **12** 408
[192] Choi S, Shin J, Park G, Eo J S, Jang J, Yang J J and Wang G 2024 3D-integrated multilayered physical reservoir array for learning and forecasting time-series information *Nat. Commun.* **15** 2044
[193] Zhu K C, Wen C, Aljarb A A, Xue F, Xu X M, Tung V, Zhang X X, Alshareef H N and Lanza M 2021 The development of integrated circuits based on two-dimensional materials *Nat. Electron.* **4** 775
[194] Xu Z *et al* 2023 Controlled on-chip fabrication of large-scale perovskite single crystal arrays for high-performance laser and photodetector integration *Light Sci. Appl.* **12** 67
[195] Novoselov K S, Mishchenko A, Carvalho A and Castro Neto A H 2016 2D materials and van der Waals heterostructures *Science* **353** aac9439
[196] Zahoor F, Zulkifli T Z A, Khanday F A, Zahoor F, Azni Zulkifli T Z and Khanday F A 2020 Resistive random access memory (RRAM): an overview of materials, switching mechanism, performance, multilevel cell (mlc) storage, modeling, and applications *Nanoscale Res. Lett.* **15** 90
[197] Ma Z, Zhang J, Lyu H, Ping X, Pan L and Shi Y 2022 Metal oxide-based photodetectors (from IR to UV) *Metal Oxides for Optoelectronics and Optics-Based Medical Applications* (Elsevier) ch 6
[198] Yu X, Marks T J, Facchetti A, Yu X, Marks T J and Facchetti A 2016 Metal oxides for optoelectronic applications *Nat. Mater.* **15** 383
[199] Qiu D, Zheng S Z and Hou P F 2024 Simulating and implementing broadband van der Waals artificial visual synapses based on photoconductivity and pyroconductivity mechanisms *ACS Appl. Mater. Interfaces* **16** 53142
[200] Liu S X *et al* 2024 Low-power perovskite neuromorphic synapse with enhanced photon efficiency for directional motion perception *ACS Appl. Mater. Interfaces* **16** 22303
[201] Jung Y, Han H, Sharma A, Jeong J, Parkin S S P and Poon J K S 2022 Integrated hybrid VO-silicon optical memory *ACS Photonics* **9** 217
[202] Kumar M, Abbas S and Kim J 2018 All-oxide-based highly transparent photonic synapse for neuromorphic computing *ACS Appl. Mater. Interfaces* **10** 34370

[203] Ostrau C, Klarhorst C, Thies M and Rückert U 2022 Benchmarking neuromorphic hardware and its energy expenditure *Front. Neurosci.* **16** 873935
[204] Hsu T H, Chen Y K, Chiu M Y, Chen G C, Liu R S, Lo C C, Tang K T, Chang M F and Hsieh C C 2021 A 0.8 V multimode vision sensor for motion and saliency detection with ping-pong PWM pixel *IEEE J. Solid-State Circuits* **56** 2516
[205] Davidson S and Furber S B 2021 Comparison of artificial and spiking neural networks on digital hardware *Front. Neurosci.* **15** 651141
[206] Peng H, Gan L, Guo X, Peng H H, Gan L and Guo X 2024 Memristor based spiking neural networks: cooperative development of neural network architecture/algorithms and memristors *Chip* **3** 100093
[207] Pfeiffer M and Pfeil T 2018 Deep learning with spiking neurons: opportunities and challenges *Front. Neurosci.* **12** 774
[208] 2024 Sony event-based sensor (available at: www.sony-semicon.com/en/products/is/industry/evs.html)
[209] 2024 PROPHESEE event based vision (available at: www.prophesee.ai/2019/07/28/event-based-vision-2/)